THE JOURNAL OF COMPARATIVE NEUROLOGY 482:123–141 (2005)

Glycinergic Neurons Expressing Enhanced Green Fluorescent Protein in Bacterial Artificial Chromosome Transgenic Mice

HANNS ULRICH ZEILHOFER,[1] BARBARA STUDLER,[2] DIMITRULA ARABADZISZ,[2] CLAUDE SCHWEIZER,[2] SEIFOLLAH AHMADI,[1] BEATE LAYH,[1] MICHAEL R. BÖSL,[3] AND JEAN-MARC FRITSCHY[2]*

[1]Department of Experimental and Clinical Pharmacology and Toxicology, University of Erlangen-Nürnberg, 91054 Erlangen, Germany
[2]Institute of Pharmacology and Toxicology, University of Zürich, 8057 Zürich, Switzerland
[3]Department of Molecular Neurobiology, Max-Planck Institute of Neurobiology, 82152 Munich-Martinsried, Germany

ABSTRACT

Although glycine is a major inhibitory transmitter in the mammalian CNS, the role of glycinergic neurons in defined neuronal circuits remains ill defined. This is due in part to difficulties in identifying these cells in living slice preparations for electrophysiological recordings and visualizing their axonal projections. To facilitate the morphological and functional analysis of glycinergic neurons, we generated bacterial artificial chromosome (BAC) transgenic mice, which specifically express enhanced green fluorescent protein (EGFP) under the control of the promotor of the glycine transporter (GlyT) 2 gene, which is a reliable marker for glycinergic neurons. Neurons expressing GlyT2-EGFP were intensely fluorescent, and their dendrites and axons could be visualized in great detail. Numerous positive neurons were detected in the spinal cord, brainstem, and cerebellum. The hypothalamus, intralaminar nuclei of the thalamus, and basal forebrain also received a dense GlyT2-EGFP innervation, whereas in the olfactory bulb, striatum, neocortex, hippocampus, and amygdala positive fibers were much less abundant. No GlyT2-EGFP-positive cell bodies were seen in the forebrain. On the subcellular level, GlyT2-EGFP fluorescence was colocalized extensively with glycine immunoreactivity in somata and dendrites and with both glycine and GlyT2 immunoreactivity in axon terminals, as shown by triple staining at all levels of the neuraxis, confirming the selective expression of the transgene in glycinergic neurons. In slice preparations of the spinal cord, no difference between the functional properties of EGFP-positive and negative neurons could be detected, confirming the utility of visually identifying glycinergic neurons to investigate their functional role in electrophysiological studies. J. Comp. Neurol. 482:123–141, 2005.

Indexing terms: glycine; glycine transporter; GlyT2; enhanced green fluorescent protein; EGFP; bacterial artificial chromosome (BAC); targeted recording; transgene

Fast inhibitory neurotransmission in the mammalian CNS is mediated by the amino acids glycine and γ-aminobutyric acid (GABA), which activate strychnine-sensitive glycine receptors and $GABA_A$ receptors, respectively. Both types of receptors permit chloride influx through the postsynaptic membrane to hyperpolarize postsynaptic neurons and to impair the dendritic propagation of excitatory postsynaptic potentials. On the cellular level, the functions of both transmitters appear closely related, yet their distributions in the mammalian CNS are very different. GABAergic neurotransmission is almost ubiquitous in the mammalian CNS, whereas glycinergic neurons are largely restricted to the spinal cord and brainstem (Zafra et al., 1997; Legendre, 2001). It is therefore not surprising that our knowledge of the contribution of

Grant sponsor: Deutsche Forschungsgemeinschaft; Grant number: Ze 377/7-1 (to H.U.Z.); Grant sponsor: Swiss National Science Foundation; Grant number: 3100-63901.00 (to J.-M.F.).

Claude Schweizer's current address is INSERM Unité 497, Ecole Normale supérieure, Biologie Cellulaire de la Synapse, 46 rue d'Ulm, 75005 Paris, France.

*Correspondence to: Jean-Marc Fritschy, Institute of Pharmacology and Toxicology, University of Zurich, Winterthurerstrasse 190, CH 8507 Zurich, Switzerland. E-mail: fritschy@pharma.unizh.ch

Received 25 June 2004; Revised 6 August 2004; Accepted 14 September 2004

DOI 10.1002/cne.20349

Published online in Wiley InterScience (www.interscience.wiley.com).

GABAergic neurons to defined neuronal circuits is much more detailed than is that of glycinergic neurons.

A major reason for our limited understanding of the contribution of glycinergic neurons to defined neuronal circuits is probably the difficulties in identifying these neurons in living, unstained brain slices to perform electrophysiological recordings. In addition, although immunoreactivity against the neuronal glycine transporter isoform (GlyT2; Liu et al., 1993) is a reliable marker for glycinergic neurons in the CNS (Poyatos et al., 1997), GlyT2 antisera label only axon terminals (Spike et al., 1997) and thus do not allow visualizing the path of glycinergic projections in the CNS. Here we report the generation of bacterial artificial chromosome (BAC) transgenic mice that express enhanced green fluorescent protein (EGFP) specifically in glycinergic neurons under the control of the GlyT2 promoter. In the CNS of these mice, numerous EGFP-expressing neurons are found throughout the spinal cord, brainstem, and parts of the cerebellum. EGFP fluorescence in these neurons extends from the somata far into dendrites and axons and even into most axon terminals. We show that EGFP expression largely overlaps with GlyT2 immunoreactivity in axon terminals and with glycine immunoreactivity in neuronal somata. In two mouse lines differing in the number of copies of the transgene, endogenous EGFP fluorescence was sufficiently bright to visualize glycinergic neurons in fixed tissue prepared for histology as well as in living, unstained spinal cord slices and thus allowed whole-cell patch-clamp recordings from visually identified glycinergic neurons.

Materials and Methods

Identification of a suitable BAC clone

A BAC clone 365E4 from the mouse C57/Bl6 BAC library RPCI-23 (Research Genetics Inc., Huntsville, AL) containing the GlyT2 (*slc6A5*) gene was identified by using the ENSEMBL database of the Wellcome Trust Sanger Institute (http://www.ensembl.org). According to this database, BAC clone 365E4 is 179,508 bp long (base 38,423,556–38,603,063 of chromosome 7) and contains the entire GlyT2 gene (from base 38,528,360 for GlyT2a or 38,528,983 for GlyT2b to 38,582,161) and an additional 105 kb and 21 kb of DNA flanking the 5′ end of exon 1 and the 3′ end of the last exon (exon 16), respectively. The presence of the entire GlyT2 coding sequence within BAC 365E4 was verified by polymerase chain reaction (PCR) and subsequent sequence analysis of exons 1 and 16.

Modification of the BAC clone

GlyT2 is expressed in the CNS in two splice variants (GlyT2a and GlyT2b), which differ in their N-termini as a result of the use of alternative first exons (exon 1a and exon 1b; Ponce et al., 1998). To allow EGFP expression independent of the use of exon 1a or 1b, we placed EGFP cDNA in frame into the beginning of exon 2 of the GlyT2 gene and removed exon 2 of the GlyT2 gene by using a two-step homologous recombination procedure (Yang et al., 1997). A targeting vector was constructed that contained the cDNA of EGFP followed by the bovine growth hormone polyadenylation (poly-A) signal (amplified by PCR from the vector pEGFP-N1; BD Bioscience Clontech, Palo Alto, CA). The EGFP-poly-A cDNA was flanked on both sides by genomic DNA homologous to 526 bp upstream and 528 bp downstream of the 5′ and 3′ ends of exon 2 of the GlyT2 gene, respectively. The Not I site located in the pEGFP-N1 plasmid between the EGFP cDNA and the poly-A was removed with Not I digestion, followed by filling of the 5′ overhanging sequence with DNA polymerase I (Klenow fragment). Homology strands were generated by using PCR with Sal I restriction sites added to the 5′ and 3′ ends of the two homology arms and a Bgl II and Pme I site added to the 5′ and 3′ ends of the 3′ homology strand (Fig. 1). This PCR product was subcloned into the PCR cloning vector pGEM-T easy (Promega, Madison, WI) and verified by DNA sequencing. The construct containing the EGFP-poly-A cDNA flanked by the two homology regions was subcloned into the Sal I site of the shuttle vector PSV1.recA, which was a generous gift from Dr. Nathaniel Heintz (Rockefeller University, New York, NY). Proper recombination after each round of homologous recombination (insertion of the targeting vector together with the shuttle vector and subsequent removal of the shuttle vector) was verified by Southern blotting with cDNA probes flanking the 5′ and 3′ homology strands. The newly introduced Pme I site, which was lost after the second recombination, was used to verify the length of the BAC DNA sequence flanking the EGFP (Fig. 1B). To exclude the presence of major undesired recombination events, restriction digestions of wild-type and modified BACs were performed with Xho I, BamH I, and Avr II (not shown).

Generation of BAC transgenic mice

For pronuclear injections, BAC DNA was purified by two rounds of CsCl gradient centrifugation, digested overnight with Not I to release the insert of genomic DNA from the BAC backbone, and diluted in injection buffer (in mM: 10 TrisCl, 0.1 EDTA, 100 NaCl, pH 7.50). A sepharose 4B (Amersham Biosciences, Buckinghamshire, United Kingdom) column was used to separate the BAC insert from the backbone. Aliquots of 0.5 ml were sampled, and the appropriate fraction for pronuclear injection was identified by using pulse field electrophoresis. Pronuclei of fertilized FVB oocytes were injected with either 1.6 or 3.0 ng/μl BAC DNA. Among 320 oocytes injected with 1.6 ng/μl DNA, 212 could be transferred into pseudopregnant mice (the remaining were lost as a result of lysis). From these, 18 mice were born, of which 8 had integrated the transgene and showed germline transmission. Among 365 oocytes injected with 3 ng/μl DNA, 272 could be transferred, 58 mice were born, and 5 had integrated the transgene and showed germline transmission. Mice derived from these oocytes were screened by PCR for the presence of EGFP and, if EGFP was present, also for the two BAC ends. Primers used for the PCRs were UZ061: 5′-CGA CGG GCA ACT ACA AGA CCG GCG/UZ063: 5′-CGA ACT CCA GCA GGA CCA TGT GAT (EGFP upstream/downstream), UZ152 5′-CAC TAA GGT TGG TGA CTT CTT CC/UZ133 5′-CTA ATA CGA CTC ACT ATA GGG AGA (T7-end upstream/downstream) and UZ153 5′-CTC ACA TAG TCC CAT CTG TTG AC/UZ 132 5′-GTC GAC ATT TAG GTG ACA CTA TA (SP6-end upstream/downstream). BAC end sequences were obtained from the TIGR BAC end database (http://www.tigr.org/tdb/humgen/bac_end_search/bac_end_search.html). Among 75 mice born, 13 were positive for EGFP. Among the 13 founders obtained, 7 were also positive of the BAC ends

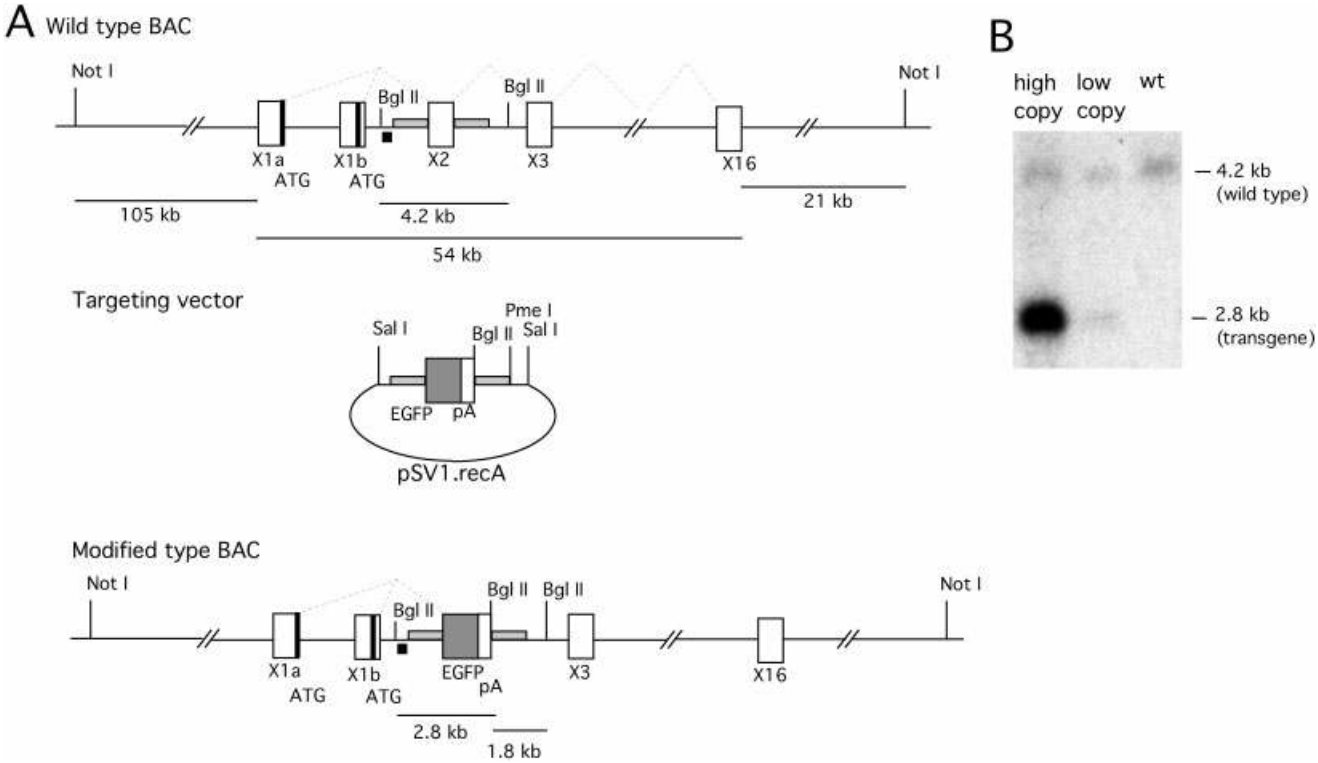

Fig. 1. Generation of BAC transgenic mice expressing EGFP in glycinergic neurons. **A:** Schematic representation of the structure of BAC 365E4 (top), of the targeting vector (middle) and of the modified BAC containing the EGFP cassette (bottom). Locations of Bgl II, Not I, and Pme I restriction sites; of the homology DNA strands used for the recombinations (light gray); and of the 5′ flanking probe (black) used for Southern blotting. **B:** Southern blot analysis of genomic DNA obtained from transgenic mouse lines 13 and 14 and from wild-type mice digested with Bgl II. High copy line 13 had multiple copies of the transgene integrated, whereas the low copy line 14 had only a single copy integrated.

(SP6 and T7) and hence had integrated the entire transgene. The lines derived from these 7 founders were expanded for further analysis. Genotyping of the mice was then done by PCR with the following primer pair, which amplified a DNA sequence spanning from intron 1 of the GlyT2 gene into EGFP (UZ 114 5′-AAT GTG TGC ATC TGT GTA TGC AGA C/UZ 064 5′-CTT GAA GAA GAT GGT GCG CTC CTG). In these mouse lines, the transgene was inherited in a mendelian manner, and transgenic mice bread and developed normally. Southern blotting was then used to estimate the number of transgenes integrated in each mouse line. A cDNA probe flanking the 5′ homology sequence located in intron 1 was generated by PCR with the following primers UZ 146 5′-CAG GAA GAT GTC AAA CGA AG (upstream) and UZ 116 5′-ACG AAT ACC TGA ACT TGA GCC TTC G (downstream). Among the 7 lines of BAC transgenic mice that had integrated the complete transgene, 2 were high copy lines with more than 4 copies integrated (line 13 and line 16), 2 had integrated a single copy (line 14 and line 15), and the rest had integrated between 2 and 4 copies. All 7 lines exhibited similar gross patterns of EGFP expression with abundant EGFP-positive neurons in the spinal cord and brainstem and only very few EGFP-positive neurons in the forebrain. In two lines, line 13 (high copy line) and line 14 (single copy line), EGFP expression was analyzed in detail. The two lines were maintained on the 129/SVJ background by crossing transgenic mice with wild type to generate heterozygote offspring. All animal experiments were approved by the local authorities and performed in accordance with the institutional guidelines of the Universities of Erlangen-Nürnberg and Zurich and the European Communities Council Directive (86/609/EEC).

Immunohistochemistry

Tissue preparation. Adult mice were deeply anesthetized with nembutal (50 mg/kg; i.p.) and perfused through the ascending aorta with 4% paraformaldehyde in 0.15 M phosphate buffer containing 15% of a saturated picric acid solution (pH 7.4). Brains were postfixed for 3 hours, cryoprotected in sucrose, frozen with powdered dry ice, and cut at 40 μm with a sliding microtome. Sections were collected in PBS and stored in an antifreeze solution (15% glucose and 30% ethylene glycol in 50 mM phosphate buffer, pH 7.4) prior to use.

Immunoperoxidase staining. Series of adjacent sections were stained for EGFP (rabbit anti-GFP cross-reacting with EGFP; 1:80,000; Synaptic Systems, Göttingen, Germany), GlyT2 (guinea pig anti-GlyT2; 1:10,000; Chemicon, Temecula, CA), glycine (rat anti-glycine paraformaldehyde conjugate; 1:10,000; gift from D. Pow, University of Queensland, Brisbane, Queensland, Australia; Pow et al., 1995), and GlyT1 (rabbit anti-GlyT1a,b; 1:30,000; gift from D. Boison, University of Zurich, Zurich,

Switzerland) to compare the regional distribution of EGFP with markers of glycinergic neurons. Free-floating sections were incubated overnight at 4°C with primary antibodies diluted in Tris buffer containing 2% normal goat serum and 0.2% Triton X-100. Sections were then washed and incubated for 30 minutes at room temperature in biotinylated secondary antibodies (1:300; Jackson Immunoresearch, West Grove, PA) diluted 1:300 in Tris buffer containing 2% normal goat serum. After three washes, sections were incubated in the ABC complex (1:100 in Tris buffer) for 20 minutes (Vectastain Elite Kit; Vector Laboratories, Burlingame, CA), washed again three times, and finally reacted with diaminobenzidine tetrahydrochloride (DAB; Sigma, St. Louis, MO) in Tris buffer (pH 7.7) containing 0.015% hydrogen peroxide. The color reaction was stopped after 10-15 minutes with ice-cold PBS. Sections were then mounted on gelatin-coated slides and air dried. Finally, they were dehydrated with an ascending series of ethanol, cleared in xylene, and coverslipped with Eukitt (Erne Chemie, Dällikon, Switzerland).

Immunofluorescence staining. The cellular and subcellular distribution of EGFP in relation to glycinergic markers was visualized by multiple immunofluorescence staining. Free-floating sections were incubated overnight in a mixture of primary antibodies (GlyT2/glycine or GlyT2/GlyT1), diluted in PBS containing 2% normal goat serum and 0.2% Triton X-100. Sections were then washed and incubated for 30 minutes at room temperature in a mixture of secondary antibodies coupled to Cy3 or to Cy5 (1:500; Jackson Immunoresearch). Sections were washed again, mounted onto gelatin-coated slides, air dried, and coverslipped with buffered glycerol. Control experiments were performed to verify that GlyT2-EGFP fluorescence was strong enough to be visualized without antibodies. EGFP-positive neurons were visualized before and after antibody staining, or EGFP immunofluorescence was detected with a red secondary antibody to distinguish it from EGFP fluorescence. In both cases, the antibody labeling did not reveal structures that were not detectable by transgenic fluorescence.

Data analysis. Sections processed for immunoperoxidase staining were analyzed with bright- and darkfield microscopy (Zeiss Axioskop, Jena, Germany) and photographed with a high-resolution color camera (Axiocam; Zeiss). Immunofluorescence staining was visualized by confocal laser scanning microscopy (Zeiss LSM-Meta) with sequential acquisition of separate color channels to avoid cross-talk between fluorochromes. For display, images were processed with the image-analysis program Imaris (Bitplane, Zurich, Switzerland).

Electrophysiology

The high copy line 13 was used for electrophysiological recordings, because EGFP-positive neurons were easier to identify in this line. Seven- to fourteen-day-old mice of either sex were killed under ether narcosis by decapitation. Transverse slices of the lumbar spinal cord 250 μm thick were prepared as described previously (Ahmadi et al., 2002). Whole-cell patch-clamp recordings were performed from neurons identified under visual control using the infrared gradient contrast technique coupled to a video microscopy system and to a CCD camera coupled to a monochromator (TILL Photonics, Gräfelfing, Germany). Slices were completely submerged and continuously superfused with external solution, which contained (in mM) 125 NaCl, 26 $NaHCO_3$, 1.25 NaH_2PO_4, 2.5 KCl, 2 $CaCl_2$, 1 $MgCl_2$, 10 glucose (pH 7.30, 315 mOsm/liter) and bubbled with 95% O_2, 5% CO_2. Patch pipettes (4–5 MΩ) were filled with internal solution containing (in mM) 130 K-gluconate, 20 KCl, 2 $MgCl_2$, 0.05 EGTA, 3 Na-ATP, 0.1 Na-GTP, 10 Na-HEPES (pH 7.30).

Results

Selective expression of EGFP in glycinergic neurons

Two lines of BAC transgenic mice, line 13 (high copy line) and line 14 (single copy line), were analyzed in detail. In both lines, a prominent EGFP fluorescence was observed in perfusion-fixed tissue sections from adult mice. It was seen in specific populations of neurons, with a heterogeneous distribution, filling their soma and dendritic tree, and in numerous axons and terminals. As expected, the highest density of labeled structures was seen in the brainstem, spinal cord, and cerebellum, whereas, in the forebrain, only certain regions contained strongly fluorescent axons and terminals. White matter tracts also contained numerous EGFP-positive fibers, especially in the spinal trigeminal tract, the brainstem reticular formation, and the lateral funiculus. In line 13, which integrated multiple copies of the transgene, the fluorescence was so intense that it masked anatomical structures, notably in the brainstem. In large neurons, in particular motoneurons, a weak EGFP signal was apparent, which could be readily distinguished from the strong fluorescence of presumptive glycinergic cells. In some presumably homozygous transgenic mice of line 13 examined initially, ectopic expression of EGFP was observed in piriform cortex and thalamus. Further analysis was therefore restricted to heterozygotes, in which this ectopic expression was not present.

A detailed immunohistochemical analysis with markers of glycinergic transmission (GlyT1a,b, GlyT2, glycine) was performed to ensure that EGFP expression was restricted to glycinergic neurons and to investigate the anatomical organization of the glycinergic system in the forebrain with this novel marker. In immunoperoxidase staining, the signal-to-noise ratio of the EGFP antibody was very high, and no staining at all was seen in nontransgenic mice (not shown). A comparison of EGFP-IR with GlyT2-IR at low magnification in adult mice revealed similar regional distribution patterns, as illustrated for line 14 in parasagittal and transverse sections of adult mouse brain (Fig. 2). The strongest staining was apparent in the brainstem, midbrain, and cerebellum. Differences in relative intensity were similar for the two markers in these regions. Staining for glycine was strongest in the regions expressing high levels of GlyT2 (and EGFP), but this marker was more widely distributed throughout the brain, in line with the ubiquitous glycine content of neurons and glial cells. GlyT1-IR partially overlapped with EGFP and GlyT2, notably in brainstem, cerebellum, and tectum, but was also very intense in regions weakly stained for these markers, such as the thalamus and olfactory bulb. In the telencephalon, notably the striatum, neocortex, hippocampal formation, and amygdala, a weak staining was observed for EGFP, GlyT2, and GlyT1, whereas glycine-IR was moderate.

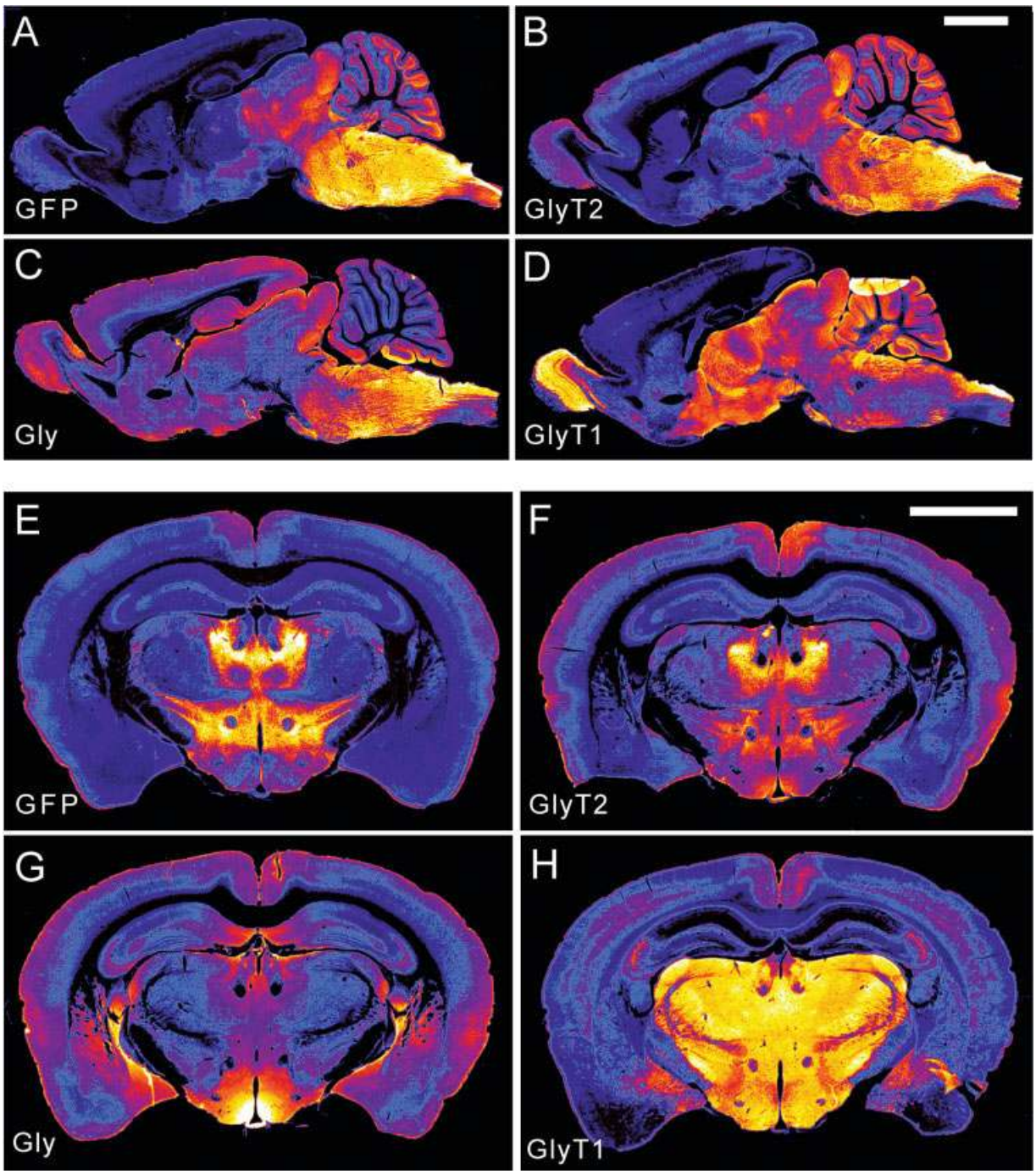

Fig. 2. Comparative distribution of EGFP (**A,E**), GlyT2 (**B,F**), glycine (Gly; **C,G**), and GlyT1 (**D,H**) in brain of adult transgenic mice (line 14), visualized by immunoperoxidase staining in parasagittal (A–D) and transverse (E–H) sections displayed in pseudocolors. The color scale was adjusted separately for each panel to maximize the regional differences in staining intensity (ranging from dark blue for background to white for maximal intensity). EGFP- and GlyT2-IR exhibit largely similar distribution patterns, although the signal-to-noise ratio is higher for EGFP. In contrast, glycine-IR has a more widespread distribution, notably in the forebrain, and GlyT1-IR overlaps only partially with EGFP. Note in particular the very intense and uniform GlyT1 staining of the diencephalon compared with the discrete distribution of EGFP and GlyT2. Scale bars = 2 mm in B (applies to A–D); 2 mm in F (applies to E–H).

A side-by-side comparison of EGFP- and GlyT2-IR at higher magnification (Figs. 3, 4) revealed an excellent correspondence for axons and terminals between the two markers, as illustrated for the thalamus and hypothalamus (Fig 3A,B). In addition, EGFP-IR, but not GlyT2-IR, was intense in the soma and dendrites of specific popula-

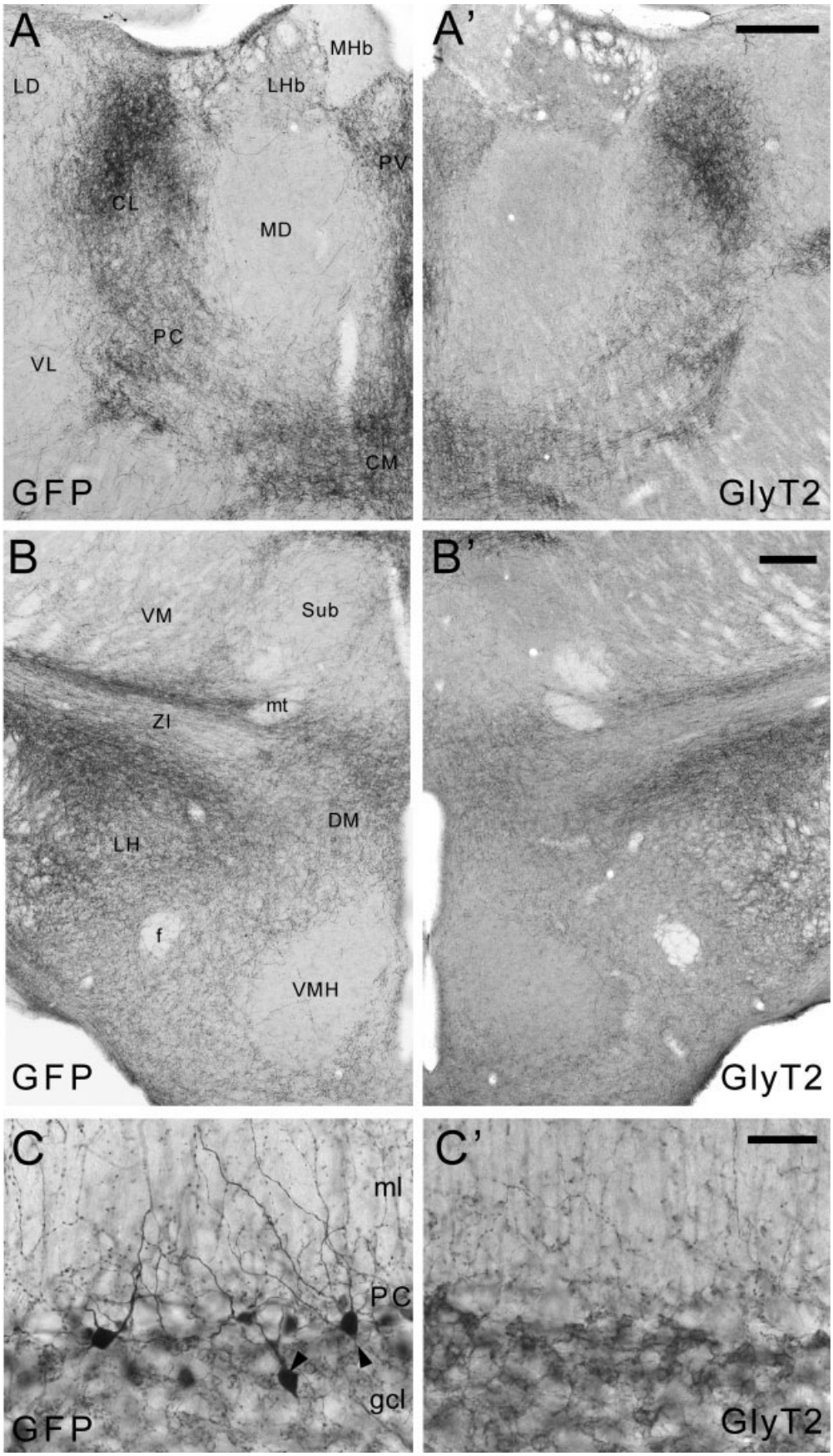
A
MHb
LD
LHb
PV
CL
MD
PC
VL
CM
GFP
A'
GlyT2
B
VM
Sub
mt
ZI
DM
LH
f
VMH
GFP
B'
GlyT2
C
ml
PC
gcl
GFP
C'
GlyT2

Figure 3

tions of neurons, as seen in the cerebellum (Fig. 3C), brainstem (Fig. 4A–E), and spinal cord (Fig. 4F,G). The regional distribution of EGFP-positive neuronal somata corresponded largely to the distribution of glycinergic neurons, as reported in the literature (Rampon et al., 1996). In the brainstem and spinal cord, both EGFP-IR and GlyT2-IR were highly abundant (Fig. 4), in line with the predominant role of glycine as an inhibitory neurotransmitter at this level of the neuraxis. As in the brain, GlyT2-IR was restricted to the neuropil, whereas numerous EGFP-positive somata were seen, notably in the reticular formation, in various nuclei of the auditory system (e.g., dorsal and ventral cochlear nuclei, superior olivary complex, nucleus of the trapezoid body), in vestibular nuclei, and in the spinal trigeminal complex (Fig. 4A–E). No staining was seen in nuclei known to be devoid of glycinergic cells, such as the inferior olive (Fig. 4D). In the spinal cord, EGFP-positive neurons were seen in laminae I, III–VIII, and X (Fig. 4F,G). A dense network of axons and terminals, producing a uniform labeling pattern at low magnification, was seen across the entire brainstem and spinal cord with both markers. In addition, EGFP-positive axons longitudinally oriented were evident in the white matter, contributing to the light coloration seen at low magnification (Fig. 4). Altogether, these findings strongly suggested that EGFP was present in glycinergic neurons characterized by expression of GlyT2. However, the differences in subcellular distribution between EGFP and GlyT2, notably as a result of the absence of detectable GlyT2 in somata, dendrites, and preterminal axons, made it more difficult to assess to what extent the transgene is selectively expressed in GlyT2-positive neurons and what proportion of glycinergic neurons expressed EGFP.

For this reason, a triple-labeling analysis was undertaken, combining EGFP with glycine and GlyT2 immunofluorescence and visualization by confocal laser scanning microscopy (Figs. 5–8). Of the three markers, EGFP was the most intense, and it filled the soma, dendritic tree, and axons, including terminals, with an intense, homogeneous fluorescence. To examine whether some EGFP might be lost during the staining procedure because of diffusion out of the cells upon permeabilization and to determine whether signal amplification with antibodies against GFP (recognizing also EGFP) was required to detect weakly labeled structures, the transgenic EGFP fluorescence was compared with the signal obtained upon immunofluorescence staining. In a first control experiment, selected cells were visualized by confocal laser scanning microscopy before and after antibody staining. As illustrated for EGFP-positive Golgi type II neurons in the cerebellum (Fig. 5A–C), even the finest processes could be seen without antibody staining, although the amplification afforded by immunofluorescence was evident, especially at the surface of the section. In a second control, EGFP immunofluorescence was detected with a red fluorescent secondary antibody (Fig. 5D). This experiment revealed that anti-EGFP antibodies do not penetrate beyond 4–6 μm into the fixed tissue section (Fig. 5D′); furthermore, they did not label more structures than seen with transgenic EGFP fluorescence (Fig. 5D,D′). Therefore, double- and triple-staining experiments with glycine and GlyT2 were performed without amplification of the EGFP fluorescence, and the analysis of colocalization patterns was restricted to the surface of the section.

Glycine staining was seen in somata and dendrites of EGFP-positive neurons, but with variable intensity. A systematic comparison of double-labeling patterns was conducted in selected regions of the brainstem (superior olivary complex, nucleus of the trapezoid body, dorsal and ventral cochlear nuclei, vestibular nuclei, pontine and medullary reticular formation, spinal nucleus of the trigeminal nerve) and cerebellum (Golgi type II cells in the granule cell layer and deep cerebellar nuclei; Figs. 6–8). In all these regions, the vast majority (>90%) of either glycine- or EGFP-positive neurons were doubly labeled. As noted above, GlyT2 staining was largely absent from neuronal somata (Fig. 6A,B), with a few exceptions as shown for the nucleus of the trapezoid body (Fig. 7A). EGFP-positive preterminal axons located in the white matter (as shown in Fig. 7E) were for the most part singly labeled; neither glycine- nor GlyT2-IR was detected. In contrast, the three markers were extensively codetected in terminal fields, as illustrated in Figure 6A,B and in Figure 7B. Glycine staining in axon terminals was granular (Figs. 6C, 7B), suggesting its presence in vesicles, whereas GlyT2-IR typically surrounded EGFP- and glycine-positive structures (Figs. 6C′, 8C3), in line with its presence in the plasma membrane. In images from triple-staining experiments, a complex mixture of colors was seen reflecting the relative staining intensity and distinct subcellular localization of the three proteins investigated (Figs. 6–8). A comparison of color-separated images (Fig. 6A1–3,C,C′) revealed that the vast majority of EGFP-positive axon terminals were positive for either glycine or GlyT2 or was triply labeled. However, the differential subcellular localization of glycine, GlyT2, and EGFP precluded a quantification of colocalization patterns, based on a pixel-per-pixel software analysis.

In the spinal cord, an extensive colocalization between EGFP and glycine or GlyT2 was also observed, in particular in axon terminals, as investigated in detail in the dorsal horn (Fig. 8). In neuronal somata, only a partial coexpression of EGFP and glycine immunofluorescence was observed. In part, this was due to the low number of EGFP-positive neurons in lamina II, where a subset of single-labeled glycine-positive neurons was observed (Fig. 8A1–3). Conversely, the number of glycine-positive neu-

Fig. 3. Comparative distribution of EGFP (**A–C**) and GlyT2 (**A′–C′**) in the thalamus (A,A′), hypothalamus (B,B′), and cerebellum (C,C′) of adult transgenic mice, as visualized by immunoperoxidase staining of transverse sections. Mirror images from hemisections are shown to facilitate the comparison. A,B: Terminal innervation fields in the thalamus and hypothalamus, where the staining of the two markers reveals highly similar distribution patterns in specific nuclei. At this forebrain level, no labeled cell bodies are present. C: Cerebellar cortex: EGFP-IR labels a population of Golgi type II interneurons in the granule cell layer (gcl) and below the Purkinje cell layer (PC; arrowheads), extending their dendrites and beaded axons into the molecular layer (ml), as well as innervating glomeruli in the gcl. In contrast, GlyT2-IR is restricted to dendrites and axons in the ml and gcl but does not label cells bodies. CL, centrolateral nucleus; CM, centromedian nucleus DM, dorsomedian hypothalamic nucleus; f, fornix; LD, laterodorsal nucleus; LH, lateral hypothalamic area; LHb, lateral habenula; MHb, medial habenula; MD, mediodorsal nucleus; mt, mammillothalamic tract; PC, paracentral nucleus; PV, paraventricular thalamic nucleus; Sub, submedius thalamic nucleus; VL, ventrolateral nucleus; VM, ventromedial nucleus; VMH, ventromedial hypothalamic nucleus; ZI, zona incerta. Scale bars = 200 μm in A,B; 50 μm in C.

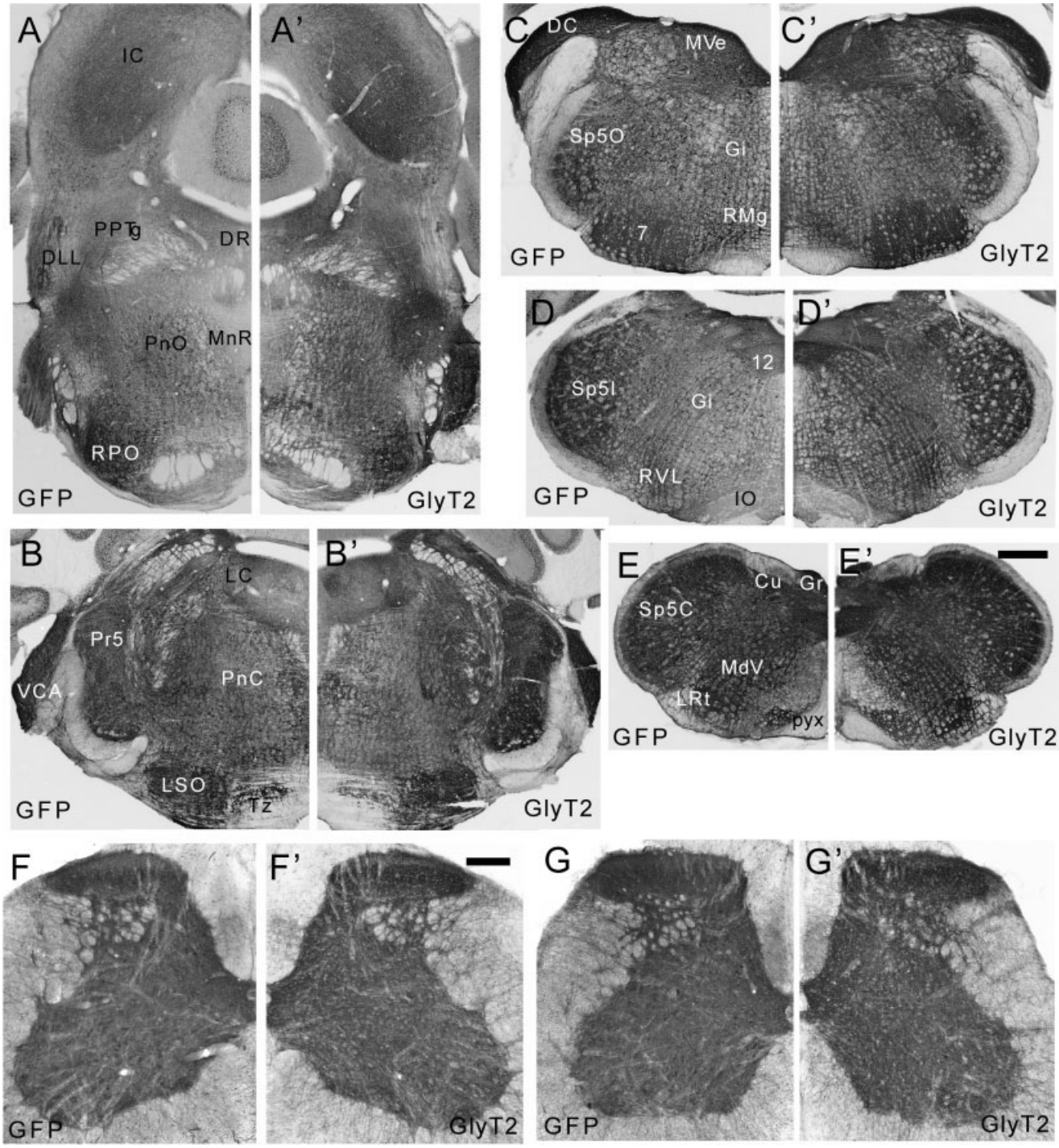

Fig. 4. Comparative distribution of EGFP (**A–G**) and GlyT2 (**A′–G′**) in the brainstem and spinal cord of adult transgenic mice, as visualized by immunoperoxidase staining of transverse sections. Mirror images from hemisections are shown to facilitate the comparison. A–E: Five levels through the pons and medulla, depicting regions containing variable densities of glycinergic neurons and terminals. At this magnification, EGFP-positive cell bodies appear as black dots. As in the forebrain (Fig. 3), the two markers exhibit remarkably similar distribution patterns, suggesting selective expression of EGFP in GlyT2-positive neurons. The relative intensity of GlyT2 staining is higher than that of EGFP in terminal fields, such as motor nuclei, reflecting the concentration of this transporter in axon terminals. F,G: Spinal cord at cervical and lumbar levels, respectively. Both markers exhibit a uniform and intense staining of the gray matter, again with a similar laminar distribution. As in brainstem, EGFP, but not GlyT2, also labels isolated cell bodies. 7, Facial nucleus; 12, hypoglossal nucleus; Cu, cuneate nucleus; DC, dorsal cochlear nucleus; DLL, nucleus of the dorsal lateral lemniscus; DR, dorsal raphe nucleus; Gi, gigantocellular nucleus; Gr, gracile nucleus; IC, inferior colliculus; IO, inferior olive; LC, locus coeruleus; LRt, lateral reticular nucleus; LSO, lateral superior olivary nucleus; MdV, ventral medullary reticular nucleus; MnR, median raphe nucleus; MVe, medial vestibular nucleus; PnC, caudal pontine nucleus; PnO, oral pontine nucleus; PPTg, peripedunculopontine tegmental nucleus; Pr5, principal trigeminal nucleus; pyx, pyramidal decussation; RVL, ventrolateral reticular nucleus; Sp5C, caudal spinal trigeminal nucleus; Sp5I, intermediate spinal trigeminal nucleus; Sp5O, oral spinal trigeminal nucleus; VCA, anterior ventral cochlear nucleus. Scale bars = 500 μm in E (applies to A–E); 200 μm in F (applies to F,G).

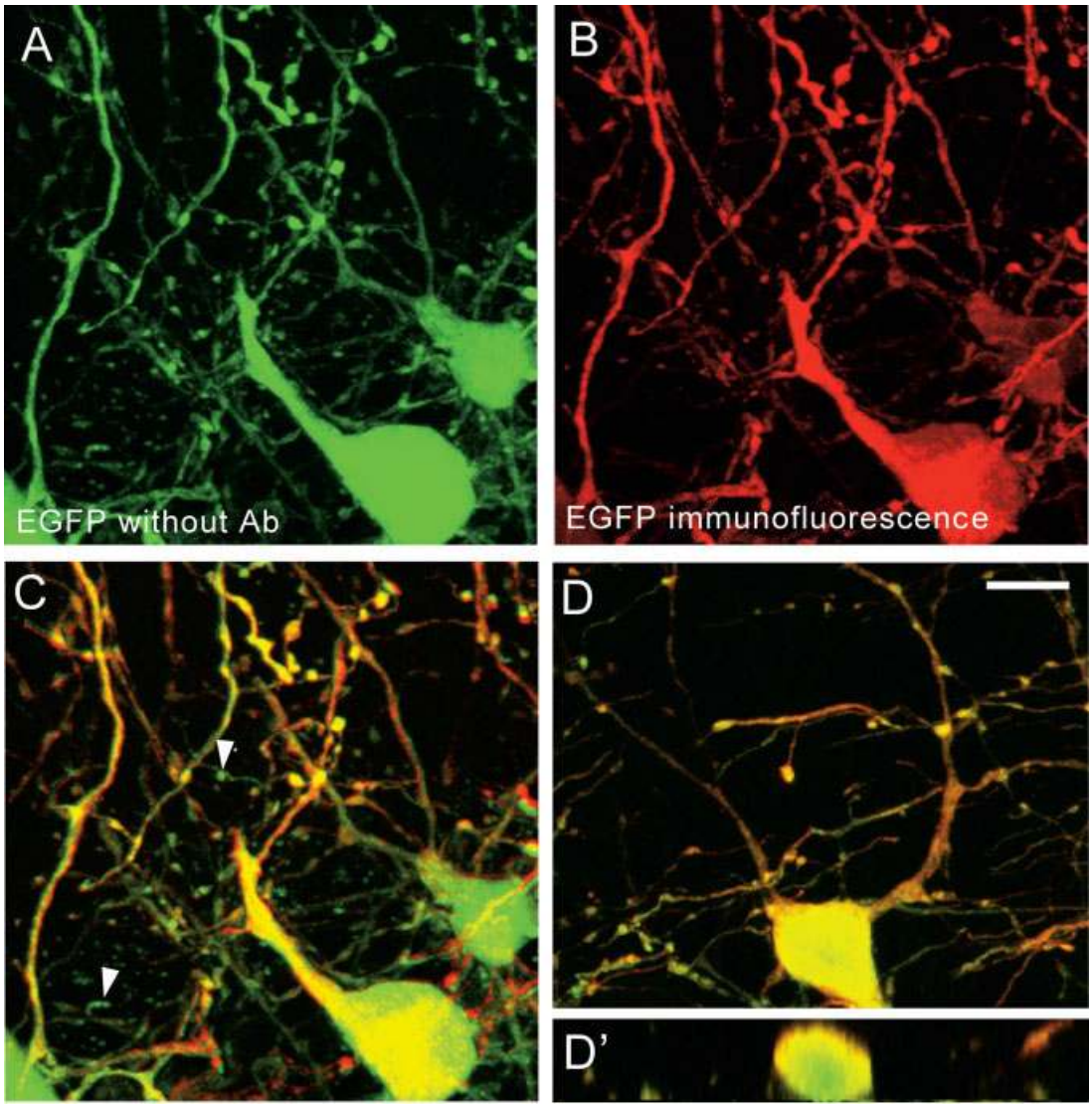

Fig. 5. Comparison of EGFP fluorescence and EGFP immunofluorescence (amplified with antibodies to EGFP), as visualized by confocal laser scanning microscopy in stacks of 24 images spaced by 0.3 μm. **A–C:** Sequential imaging of the same Golgi type II cells in the cerebellum before (A; green) and after immunofluorescence staining (B; red color coding). In B, the signal was a composite of EGFP fluorescence and of the immunofluorescence emitted by the secondary antibody; it is shown in red to facilitate the comparison with A. In C, the two panels are superimposed; yellow denotes the nearly identical distribution of the EGFP fluorescence and immunofluorescence. The green neurites (arrowheads) and cell bodies are located deep in the section, indicating a limited penetration of the antibodies against EGFP. **D:** GlyT2-EGFP fluorescence of a cell (green) and the corresponding EGFP immunofluorescence (red), detected with a secondary antibody conjugated to a red fluorochrome; the corresponding images are superposed to demonstrate the overlap between the two signals; in **D′**, the stack of images is depicted along the z-axis to illustrate the reduced penetration of the EGFP antibodies into the section, resulting in a gradual decrease of the red signal. Also note that the antibodies do not penetrate inside the cell body. Scale bar = 10 μm.

rons in laminae III and IV was rather variable from section to section, and even when comparing the left and right sides of a given section. The causes for this variability are not known, but it was seen also in nontransgenic mice from the same litters (not shown). In spite of this variability, the great majority of EGFP-positive axon terminals in laminae I–IV were doubly labeled either with glycine or with GlyT2 (Fig. 8B1–3). Given the selective localization of the latter marker in axon terminals, EGFP-positive axons appeared either doubly or triply labeled. The superficial, presumably membrane-bound, localization of GlyT2 immunofluorescence compared with EGFP was best seen in lamina II, which contains a lower density of terminals than the deeper laminae (Fig. 8C3).

Double-immunofluorescence staining between EGFP and GlyT1, the glial glycine transporter, revealed that the two markers were completely separated at all levels of the neuraxis. This is illustrated for the tectum, the granule cell layer of the cerebellum, and the spinal cord lateral funiculus (Fig. 7C–E). GlyT1-IR was extremely abundant in these areas, labeling a fine and profuse network of filamentous structures, likely representing astrocytic pro-

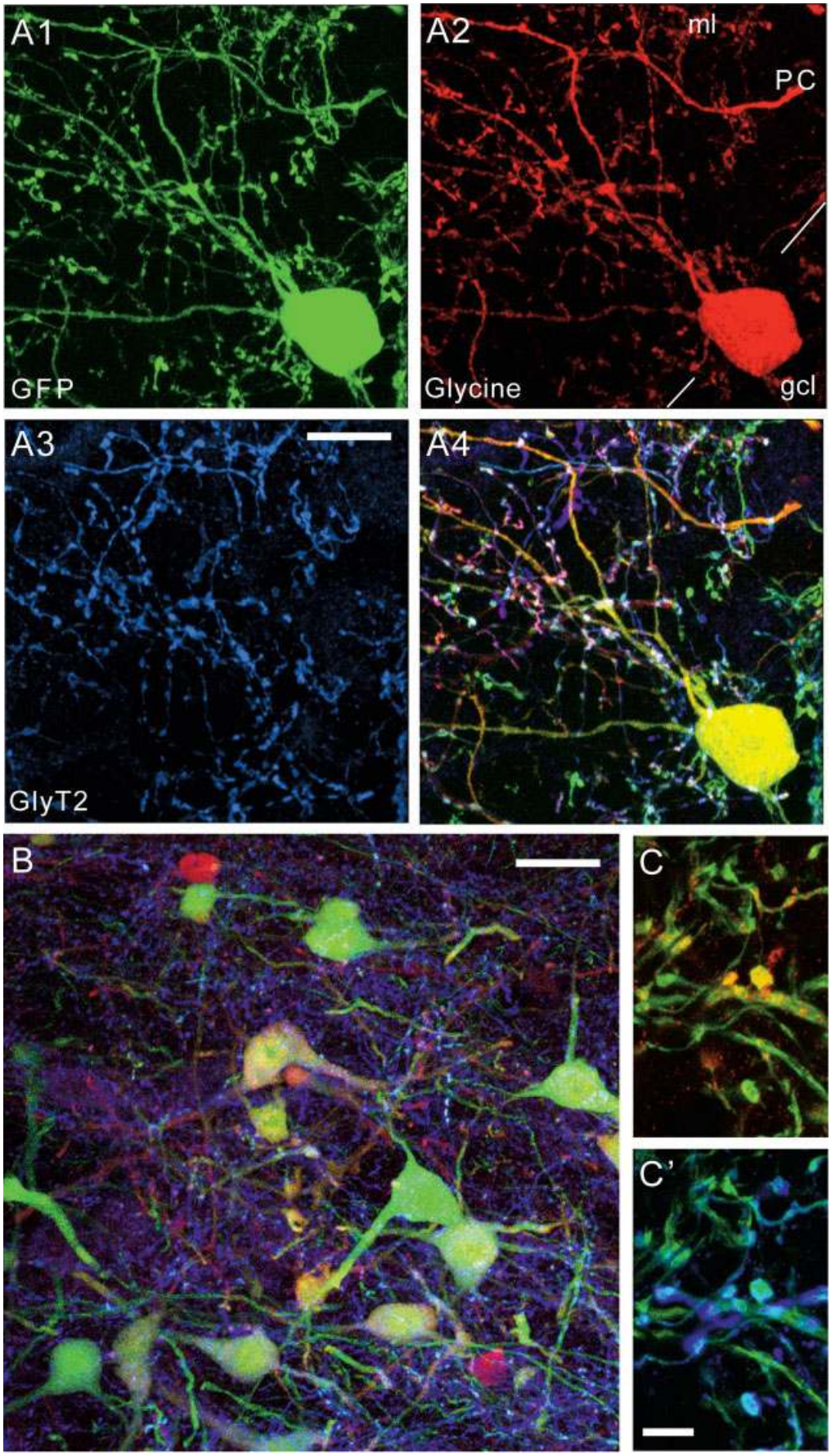

Figure 6

cesses. They often were close to EGFP-positive axon terminals, somata, and dendrites, but no colocalization was apparent, suggesting that EGFP was strictly expressed in neurons (Fig. 7C–E). In the brainstem and spinal cord, numerous white matter tracts contained EGFP-positive axons. While these fibers were mixed with GlyT1-positive processes (Fig. 7E), they typically lacked GlyT2-IR (not shown).

Anatomical organization of the glycinergic system in forebrain

The high sensitivity and signal-to-noise ratio of EGFP in transgenic mice provided a unique opportunity to investigate the anatomical organization of the glycinergic system in the brain (Fig. 9). Although glycine itself has been studied extensively in the brainstem and spinal cord, much less is known about its distribution in the forebrain (van den Pol and Gorcs, 1988; Rampon et al., 1996). As shown in Figures 2 and 3, specific forebrain areas received a dense innervation of EGFP-positive axons and terminals. The most rostrally located cells were seen in the posterior hypothalamus (Fig. 9), in the deep layers of the inferior colliculus, and in the midbrain tegmentum. The distribution of EGFP-positive fibers and terminals in major areas of the forebrain is summarized in Table 1, with a distinction of innervation density (ranging from 0 to 5) and type of terminal varicosities, as illustrated in Figure 10.

EGFP-positive fibers entered the forebrain along the medial forebrain bundle, crossing the hypothalamus, where numerous terminal fields were identified (Figs. 3B, 9F,G), and extended toward the thalamus and the basal forebrain (Fig. 9E,H). A few EGFP-positive axons could be traced around the rostrum of the corpus callosum, extending into frontal and cingulate cortex, and caudally, entering the hippocampal formation. Some axons were seen also in the internal capsule, forming isolated terminal branches with varicosities in the most dorsal part of the striatum, just bellow the cortical white matter. Other EGFP-positive axons entered the external capsule or even the optic tract. In the thalamus, the major glycinergic innervation was seen in intralaminar nuclei, notably the centrolateral and centromedial nuclei. The reticular nucleus of the thalamus received a moderate innervation, except in its dorsal part, which was densely populated by EGFP-positive fibers (Fig. 9D).

The most rostral fibers extended into the anterior olfactory nucleus, but only very few, isolated axons could be traced into the granule cell layer of the olfactory bulb. Compared with the diencephalon (thalamus, hypothalamus), only the basal forebrain contained a relatively high density of EGFP-positive axons, notably in the medial septum, the nucleus of the diagonal band of Broca, and the substantia innominata (Fig. 9E,H), suggesting interactions between glycinergic and cholinergic transmission. In the remaining telencephalon, the innervation density was either sparse or nearly absent. In the basal ganglia, for example, only the medial portion of the globus pallidus and the central nucleus of the amygdala received a moderate innervation (1–2 on a scale of 5). All other nuclei ranged between 0 and 1.

The regions receiving the most widespread innervation from EGFP-positive axons and terminals were the preoptic area and the hypothalamus. As in other forebrain regions, the distribution was highly specific and different across distinct nuclei (Figs. 3B, 9, Table 1), indicating that glycinergic input differentially modulates various hypothalamic centers.

At higher magnification, a clear distinction could be made between preterminal axons, which were smooth and of regular diameter, and axon terminals, which appeared either varicose or formed numerous short terminal branches ending with a bouton (Fig. 10). The size of these varicosities and boutons was rather varied, depending on the region innervated (Table 1).

Active and passive membrane properties of glycinergic dorsal horn interneurons

To determine whether glycinergic neurons, recognized by EGFP expression, have specific functional properties, we next characterized passive membrane properties and firing patterns of these cells in the spinal cord. In heterozygote mice of the high copy line (line 13), native EGFP fluorescence was sufficiently bright to allow whole-cell patch-clamp recordings from identified glycinergic neurons in 250-μm-thick living spinal cord slices (Fig. 11A,B). Recordings were made from a total of 50 (28 EGFP-positive and 22 EGFP-negative) neurons in the superficial laminae (I–III) of the spinal cord dorsal horn. Passive membrane properties determined in the current-clamp mode were nearly identical in EGFP-positive and -negative neurons (Table 2). To characterize the firing pattern, depolarizing current injections of increasing amplitude and lasting for 1 second were applied from a resting potential adjusted to –70 ± 5 mV. In most (15 of 28) EGFP-positive neurons, suprathreshold depolarization elicited continuous trains of action potentials through the entire depolarization period with no or only very little frequency adaptation. These neurons were classified as tonic firing (Fig. 11C). Most of the remaining neurons (9/28) fired either one or two action potentials at the beginning of the depolarization and were classified as singly spiking neurons (Fig. 11D). Two other firing patterns, phasic with one or more short trains of action potentials separated by silent periods or delayed firing with the first action potentials occurring after a delay (of at least 150 msec), occurred much less frequently (3/28 and 1/28, respectively). Only two neurons exhibited a gap-firing pattern (Ruscheweyh et al., 2004), characterized by a significant delay between the first and second action potentials (Fig. 11E). Both of these neurons were EGFP

Fig. 6. Identification of EGFP-positive neurons (A1, green) as glycinergic by triple-immunofluorescence staining with glycine (A2, red) and GlyT2 (A3, blue) in the cerebellum of adult transgenic mice. **A1–A4:** Golgi type II cell located just below the Purkinje cell layer (PC) exhibits an intense glycine immunofluorescence in its soma, dendrites, and some axons. Most EGFP-positive processes in the molecular layer (ml) and granule cell layer (gcl) are also labeled with GlyT2, indicating that they are glycinergic. In the overlay (A4), the various colors indicate the degree of double and triple labeling. **B:** A group of glycinergic neurons in the deep cerebellar nuclei, seen in a triple-labeled image. These cells express a variable intensity of glycine staining in their soma and dendrites. **C,C′:** Enlargement of dendrites and axons, illustrating two combinations of double labeling (EGFP-glycine and EGFP-GlyT2, respecitively). Glycine-IR (red) typically appeared granular in dendrites and axons. In contrast, GlyT2 staining (blue) appeared to surround some EGFP-positive axons (green), representing presumably terminal fibers. Scale bars = 20 μm in A,B; 10 μm in C.

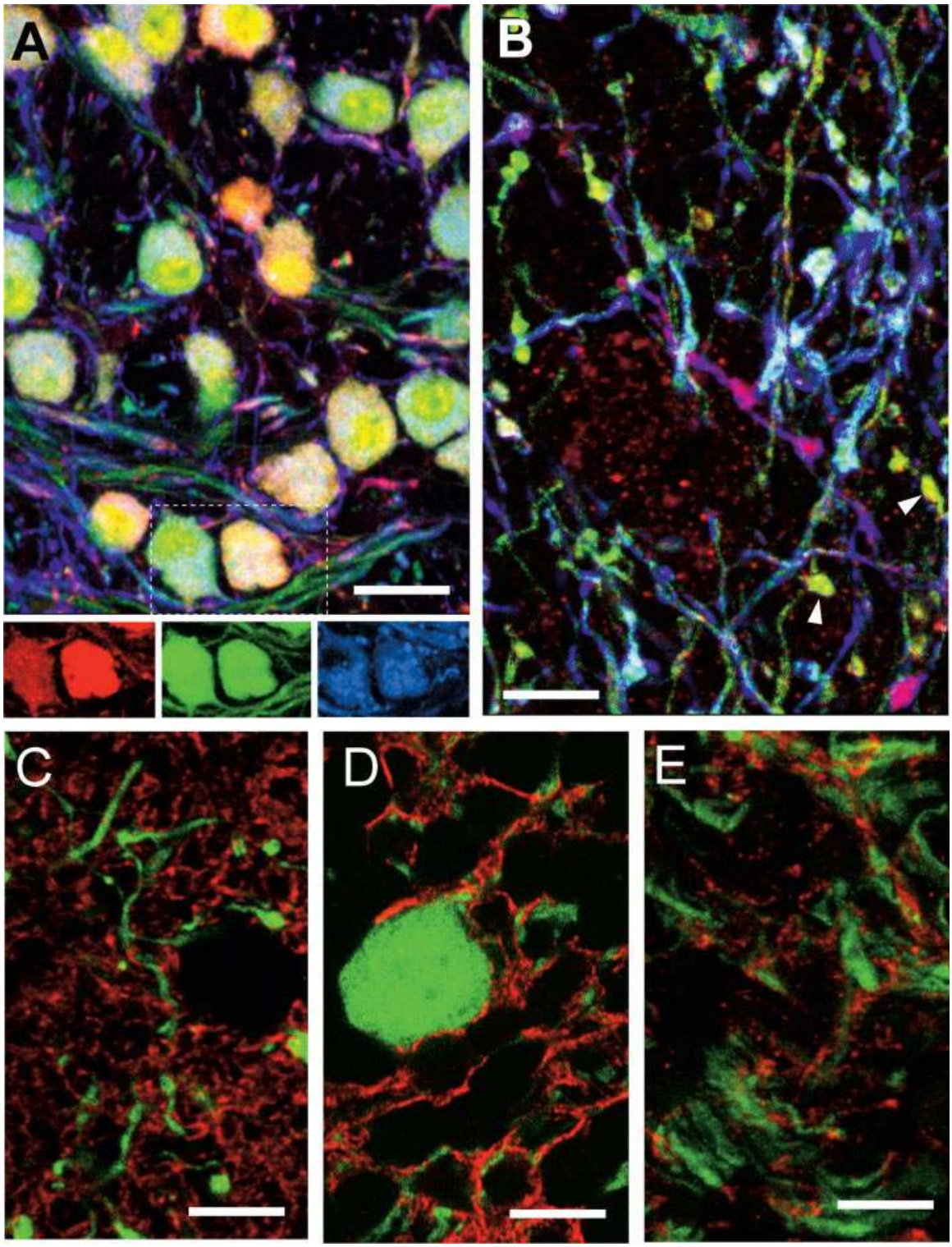

Fig. 7. Identification of EGFP-positive neurons and axons (green) as glycinergic by triple-immunofluorescence staining with glycine (red) and GlyT2 (blue) in the brainstem of adult transgenic mice. **A:** Nucleus of the trapezoid body, shown by overlay of the three markers. The **insets** display color-separated panels. As in the cerebellum, changing intensities of staining for each marker result in a complex color pattern, but nearly every EGFP-positive structure is colocalized either with glycine or with GlyT2 or with both. **B:** Terminal innervation field in the medullary reticular formation. EGFP-positive axons typically form varicosities of variable size. Many of them are surrounded by GlyT2 labeling and contained glycine. Note that glycine is sometimes present in EGFP-positive axons in places lacking GlyT2 (arrowheads). **C–E:** Distinct cellular localization of EGFP and GlyT1 illustrated by double immunofluorescence in three distinct brain regions. C: In the pretectal area, EGFP-positive axons are embedded in a dense network of GlyT1-positive processes (presumably from astrocytes). D: In the granule cell layer of the cerebellum, GlyT1-positive processes likewise closely surround an EGFP-positive neuron and its dendrites. E: In the lateral funiculus of the cervical spinal cord, EGFP-positive axons cut in cross-section are intermingled with very fine GlyT1-positive structures. No colocalization of the two markers was ever observed. Scale bars = 20 μm in A; 10 μm in B–E.

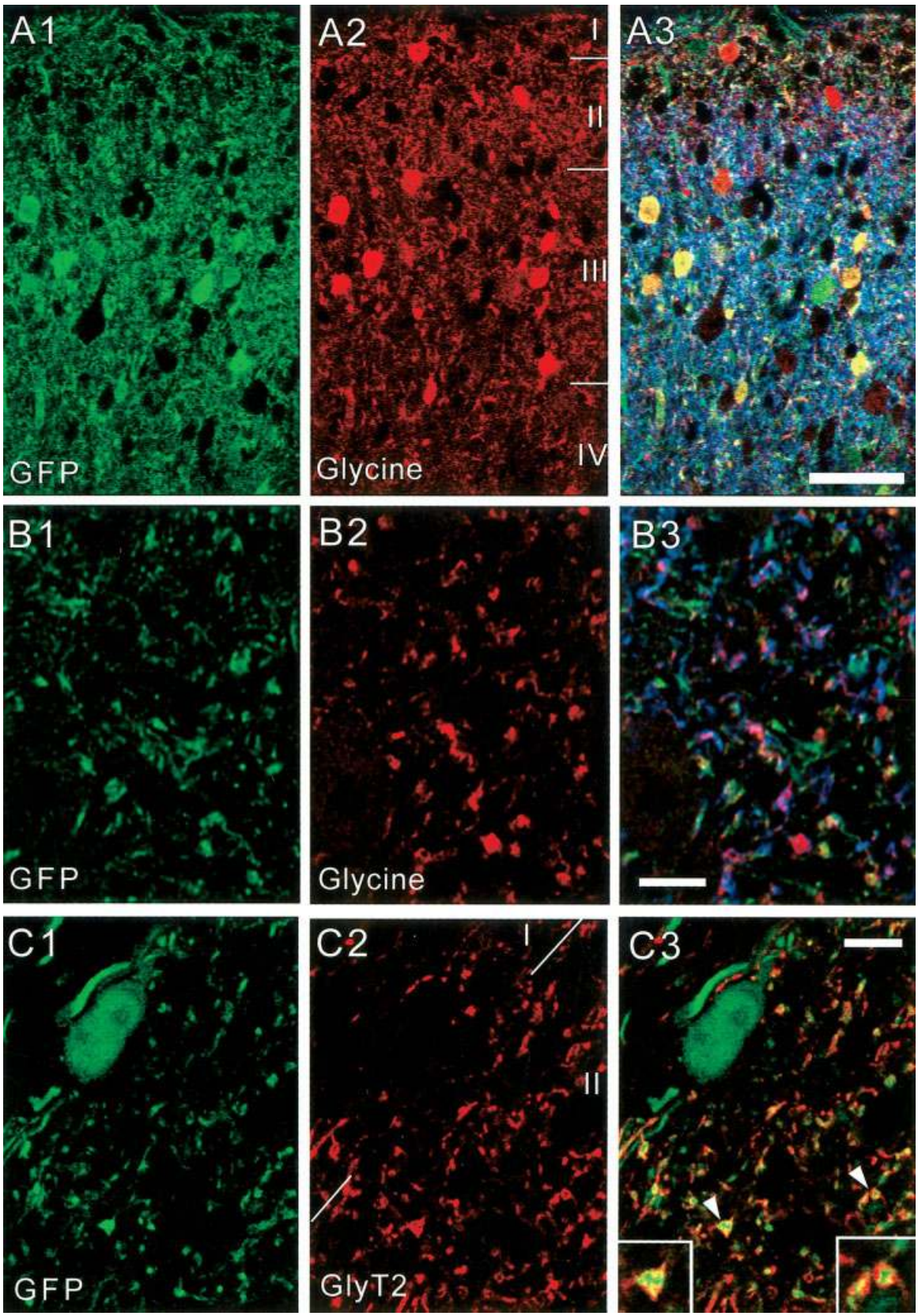

Fig. 8. Identification of EGFP-positive neurons as glycinergic in the superficial laminae of the spinal cord. **A1–A3:** Triple immunofluorescence staining of laminae I–IV of the lumbar dorsal horn with EGFP (green), glycine-IR (red), and GlyT2 (blue), seen at low magnification in color-separated images (A1,A2) and in the overlay (A3). Note that glycinergic neurons in lamina II apparently lack EGFP in their soma. **B1–B3:** High-magnification images of axons in lamina II. The great majority of green axons are doubly labeled with glycine, and many of them are surrounded by GlyT2-IR. **C1–C3:** Double immunofluorescence for EGFP (C1) and GlyT2 (C2) in laminae I–II of cervical dorsal horn, shown in color-separated images and in the overlay (C3). An EGFP-positive neuron present in lamina I lacks GlyT2-IR. In lamina II, green axons are doubly labeled or appear surrounded with GlyT2-IR, as illustrated in the **insets** for two examples indicated by arrowheads. Scale bars = 30 μm in A; 5 μm in B; 10 μm in C.

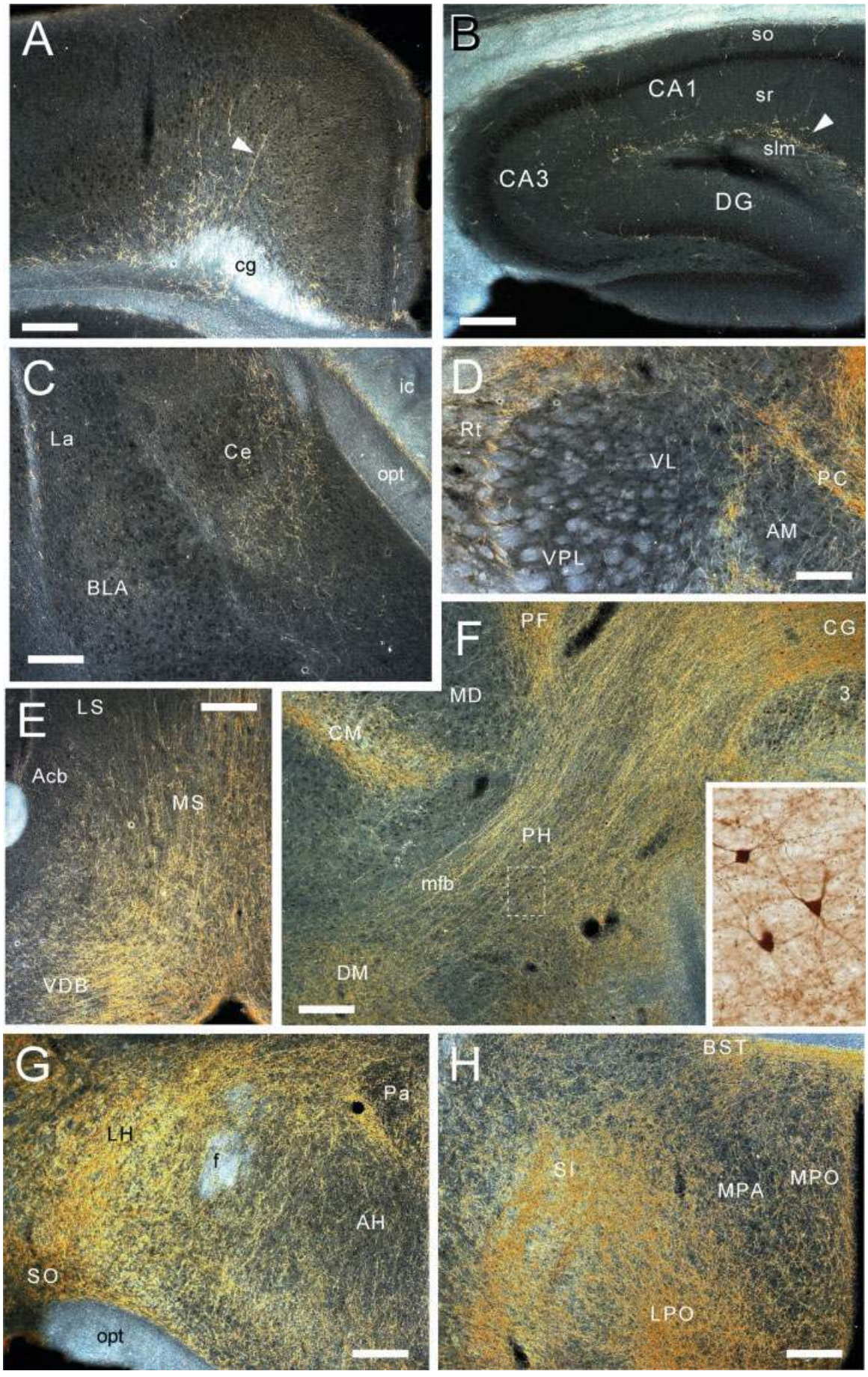
A
cg
B
so
CA1
sr
slm
CA3
DG
C
ic
La
Ce
opt
BLA
D
Rt
VL
PC
AM
VPL
E
LS
Acb
MS
VDB
F
PF
CG
MD
3
CM
PH
mfb
DM
G
Pa
LH
f
AH
SO
opt
H
BST
SI
MPA
MPO
LPO

Figure 9

negative and located in lamina II and III. Apart from this observation, no significant differences in the frequency of the different firing patterns were seen between EGFP-positive and -negative neurons (Tables 2, 3).

Discussion

Intense and stable expression of EGFP localized to specific neuronal populations can be achieved by using BAC transgenes to allow functional and morphological analysis of defined neurotransmitter systems (Heintz, 2001; Meyer et al., 2002; Gong et al., 2003). The present study demonstrates that this strategy can be applied successfully for the study of glycinergic neurons, based on the selective expression of GlyT2 in these cells (Jursky and Nelson, 1995; Zafra et al., 1995; Poyatos et al., 1997; Spike et al., 1997). Several lines of evidence support the conclusion that EGFP was selectively expressed by glycinergic neurons in both lines of transgenic mice examined: 1) The regional distribution of EGFP-positive cells overlaps precisely with the known distribution of glycinergic neurons (van den Pol and Gorcs, 1988; Rampon et al., 1996; Tanaka and Ezure, 2004); 2) the vast majority of EGFP-positive cells were strongly immunoreactive for glycine; 3) GlyT2 staining selectively surrounded EGFP-positive terminals; and 4) GlyT1-positive processes were always devoid of EGFP fluorescence. The exquisite morphological details revealed by EGFP therefore provide a unique view of the organization of the glycinergic system in the mouse. Because GlyT2-IR does not label the majority of glycinergic cell somata, and because glycinergic neurons cannot be identified unambiguously by their functional properties, as shown here for the spinal cord (Tables 2, 3), it is a major advantage to be able to visualize them directly in vivo and in vitro.

Methodological considerations

The two lines of mice investigated differed in the number of copies of the transgene integrated in their genomes. Whereas multiple copies in line 13 give rise, as expected, to a stronger EGFP expression, a single copy was sufficient for histological analysis. While differing in intensity, the two lines exhibited similar regional patterns of EGFP fluorescence, suggesting that a single copy of the transgene was sufficient to achieve the complete pattern of expression under control of the GlyT2 gene promotor, independently of the insertion site. A potential concern was that certain glycinergic structures might remain undetected because of insufficient transgene expression. Our control experiments (Fig. 4) demonstrate, however, that, in the single-copy line, amplification with EGFP immunofluorescence was not required to visualize EGFP even in the finest axonal process. On the contrary, immunofluorescence was limited by the penetration of the antibodies into the fixed tissue section. The single copy line was preferred for histological analysis, because the stronger EGFP expression of line 13 resulted apparently in some leakage of EGFP upon tissue fixation, freezing, and permeabilization, which masked the cytoarchitecture at low magnification. This was verified in control experiments using 12-μm sections from fresh-frozen tissue, in which EGFP fluorescence became uniformly distributed within a few hours after sectioning. To overcome such limitations, a modified form of EGFP, for example, membrane-anchored EGFP, might be more suitable in the future. In contrast, the strong fluorescence seen in mice from line 13 allowed easy identification of positive cells in living slices prepared for electrophysiological analysis (Fig. 11), thereby ensuring effective sampling of glycinergic neurons.

The use of BAC clones for the generation of transgenic mice permits the integration of very large fragments of foreign DNA into the mouse genome. These fragments are sufficiently large to host most, if not all, regulatory elements of a given gene. Nevertheless, it cannot be excluded that some regulatory elements may be missing in a specific construct or that regulatory elements neighboring the integration site of the transgene affect its expression. It is therefore still essential to verify that expression of the EGFP transgene is eutopic. Three markers, differing in subcellular localization, were required to analyze the pattern of EGFP expression relative to glycinergic neurons. Several lines of evidence indicate that ectopic (or partial) expression of the transgene was unlikely in both lines of mice. A side-by-side comparison of EGFP and GlyT2 staining (Figs. 3, 4) revealed the excellent correspondence of the distribution of labeled axons in forebrain, brainstem, and spinal cord and indicated that the transgene is ex-

Fig. 9. Regional distribution of EGFP-positive axons in the forebrain of adult transgenic mice, as visualized by darkfield imaging of sections processed for immunoperoxidase staining. A, C–E, G, and H are taken from transverse sections, B and F from parasagittal sections. Labeled axons appeared yellow-gold, gray matter dark gray-blue, and white matter light gray-blue. **A:** Cingulate cortex: fibers emerging from the cingulum (cg) extend toward the surface of the cortex (arrowhead). **B:** Hippocampal formation: a moderate innervation is localized in the stratum lacunosum-moleculare (slm) of CA1 and a few isolated fibers are seen in CA1 and CA3 and in the hilus of the dentate gyrus (DG). **C:** Amygdala: the central nucleus (Ce) receives a light innervation from EGFP-IR axons. Note the presence of numerous fibers between the internal capsule (ic) and the optic tract (opt). La, lateral amygadala; BLA, basolateral amygdala. **D:** Dense innervation of thalamic intralaminar nuclei and the dorsal part of the reticular nucleus (Rt). Note fibers crossing the anteromedial nucleus (AM) to enter the paracentral nucleus (PC). The ventrolateral nucleus (VL) and ventroposterolateral nucleus (VPL) are almost devoid of innervation by EGFP-positive fibers. **E:** Medial septum (MS) and nucleus of the diagonal band of Broca (VDB): a dense terminal field is evident in this region, emerging ventrolaterally from the medial forebrain bundle. Note that the nucleus accumbens (Acb) and lateral septum (LS) contain very few positive fibers. **F:** EGFP-positive axons in the medial forebrain bundle (mfb), crossing the posterior hypothalamus (PH) and entering the thalamus; several terminal fields with a dense innervation are evident in the central gray (CG) above the oculomotor nucleus (3), the parafornical nucleus of the thalamus (PF), the centromedian nucleus of the thalamus (CM), and the dorsomedial nucleus of the hypothalamus (DM); in contrast, the mediodorsal nucleus of the thalamus (MD) is free of EGFP staining. The **inset** shows by brightfield microscopy the presence of isolated neurons; these cells are among the most rostrally located EGFP-positive cells in the forebrain. **G:** Dense GlyT2-EGFP innervation of the hypothalamus. Ascending fibers cut in cross-section are most numerous in the lateral hypothalamic area (LH). Note how the paraventricular nucleus (Pa) is surrounded by EGFP-positive fibers. f, Fornix; AH, anterior hypothalamic area. **H:** Dense terminal innervation fields in the preoptic area. The medial preoptic nucleus (MPO) and medial preoptic area (MPA), like the anterior hypothalamus in G, receive a moderate innervation. In contrast, the lateral preoptic nucleus (LPO), the substantia innominata (SI), and the bed nucleus of the stria terminalis (BST) are densely innervated. Scale bars = 200 μm in A–D,F–H; 100 μm in E.

TABLE 1. Regional Distribution of EGFP-Positive Axons in the Forebrain Assessed Visually in Sections Processed for Immunoperoxidase Staining With Antibodies to EGFP[1]

Region	Layer/nucleus	Density of axons terminals	Size of varicosities
Olfactory bulb	Glomeruli	0	—
	Mitral cells, EPL	0	—
	Granule cell layer	0–1	2
Cerebral cortex	Frontal, motor	1 (layer 6)	1–2
	S1	1 (layer 6)	1–2
	V1	1 (all layers)	1
	Cingulate	1–2	1
	Piriform	1	1
	Entorhinal	1	1
Hippocampal formation	CA1	1 (so), 2 (slm)	1
	CA3	1 (so, sr), 2 (slm)	1
	Hilus	0–1	1
	Dentate gyrus	0–1 (gcl)	1
	Subiculum	2–4	1
	Parasubiculum	1	1
Basal forebrain	Medial septum	3–4	1
	Lateral septum	0–1	1
	Diagonal band of Broca	3	1
	Bed n. stria terminalis	4	2–3
	N. Stria medullaris	4	3
	Subst. innominata	3–5	1–3
Basal ganglia	Striatum	0–1	1
	N. accumbens	0	—
	Olfactory tubercle	0	—
	Globus pallidus	1 (lateral), 2 (medial)	1
	Interpeduncular n.	0	—
	Subthalamic n.	0	—
	Substantia nigra compacta	1	1
	Substantia nigra reticulata	0	—
Amygdala	Central	1	1
	Lateral	0–1	1
	Basal	0–1	1
	Medial amygdaloid n.	1	1
Thalamus	Anterior nuclei	0	—
	Reticular n.	1 (ventral), 3 (dorsal)	1
	Ventral anterior n.	1	1
	Ventral lateral n.	1	1
	Ventral posterior n.	1	1
	Lateral ventral n.	1	1
	Lateral posterior n.	2	1–3
	Lateral dorsal n.	1	1–3
	Posterior thalamus	1–2	1–3
	Dorsal lateral geniculate n.	0–1	1
	Ventral lateral geniculate n.	2	2
	Medial geniculate n.	0–1	1
	Paracentral n.	4	3
	Centromedian n.	3–5	1–3
	Mediodorsal n.	1	1
	Centrolateral n.	5	1–3
	Parafascicular n.	5	1–3
	Reuniens n.	5	1–3
	Paraventricular n.	4	1
	Lateral habenula	2	1
	Medial habenula	0	—
	Zona incerta	4–5	1
	Pretectal area	4–5	1–3
Hypothalamus	Medial preoptic area	2	1–2
	Lateral preoptic n.	4	1–3
	Anterior hypothalamic area	2	1–3
	Lateral hypothalamus	3	1–3
	Suprachiasmatic n.	0	—
	Supraoptic n.	1	2
	Paraventricular n.	1–3	1–3
	Periventricular n.	2	2
	Tuber cinereum	3	1
	Ventromedial n.	0–1	1
	Dorsomedial n.	2	1–2
	Arcuate n.	1–2	1
	Median eminence	0	—
	Mammillary bodies	0–1	1
	Posterior hypothalamus	2–4	1–3

[1]The scaling of innervation density ranges from 0 (no labeled axons) to 5. Three classes of varicosities were determined, corresponding to small, medium-sized, or large, as illustrated in Figure 10. gcl, Granule cell layer; n., nucleus; slm, stratum lacunosum-moleculare; so, stratum oriens; sr, stratum radiatum.

pressed in all regions containing GlyT2-positive structures. Moreover, in the absence of GlyT2-IR in the soma and dendrites of most glycinergic neurons, the use of glycine proved useful, although the expression level was highly variable from section to section, and most preterminal axons, notably in the white matter, were devoid of either glycine- or GlyT2-IR. For these reasons, no attempt was made to quantify the extent of colocalization between EGFP and glycine or GlyT2. Instead, we selected to examine systematically various brain areas known to contain glycinergic neurons and axon terminals (Figs. 6, 7). The results provide strong evidence for a selective expression of EGFP in most glycinergic neurons. Some discrepancies nevertheless were seen in the spinal cord, where EGFP-positive cells devoid of glycine staining, or vice versa, were observed, in particular in laminae I and II. It should be noted, however, that previous studies have reported a pattern of glycine-IR in these laminae that is much closer to the present EGFP pattern (Todd and Sullivan, 1990; van den Pool and Gorcs, 1998). We therefore believe that these discrepancies are of a technical nature and reflect natural variations in the extent of glycine-IR in spinal cord neurons.

GlyT1 staining was used to rule out expression of EGFP in astrocytic processes. GlyT1 is selectively expressed in astrocytes (Adams et al., 1995; Zafra et al., 1995), although early studies had reported GlyT1 mRNA expression in both astrocytes and neurons (Smith et al., 1992; Borowsky et al., 1993). In the present study, the GlyT1 antibody directed against the C-terminal portion of this protein (which recognizes both GlyT1a and GlyT1b) selectively labeled only astrocytes and their processes, with striking regional differences, as shown in Figure 2. The complete lack of colocalization between EGFP and GlyT1-IR provides compelling evidence that expression of the transgene is strictly neuronal.

Anatomical organization of the glycinergic system

Most of the knowledge of the anatomical organization of neurochemically defined neurons, such as GABAergic neurons, is derived from the analysis of unrelated markers, including neuropeptides, calcium-binding proteins, or specific enzymes, expressed in these neurons (Freund and Buzsaki, 1996). Such markers have not been identified for most glycinergic neurons, so little is known about the organization of glycinergic circuits, notably in the forebrain. This issue is of major relevance, in that the distribution of glycine receptor subunits is more widespread (Araki et al., 1988; Malosio et al., 1991) than that of glycinergic axon terminals, as shown here. The present mice, therefore, represent a powerful tool for future functional studies of the role of glycinergic projections in the CNS. Although the cellular and regional distribution of GlyT2 has been described (Jursky and Nelson, 1995; Zafra et al., 1995; Poyatos et al., 1997; Spike et al., 1997; Tanaka and Ezure, 2004), the resolution and sensitivity of the present approach considerably extends these previous observations, notably by labeling glycinergic neurons entirely, including their preterminal axon. The prominent labeling of longitudinal fibers in the lateral and dorsal funiculi, as well as in the brainstem, is harmonious with the demonstrations of descending glycinergic projections from the brainstem (Antal et al., 1996).

For the forebrain, our results confirm the presence of glycinergic axons, notably in the hypothalamus, thalamus, and basal forebrain (Rampon et al., 1996). They also provide unambiguous evidence for the absence of glycin-

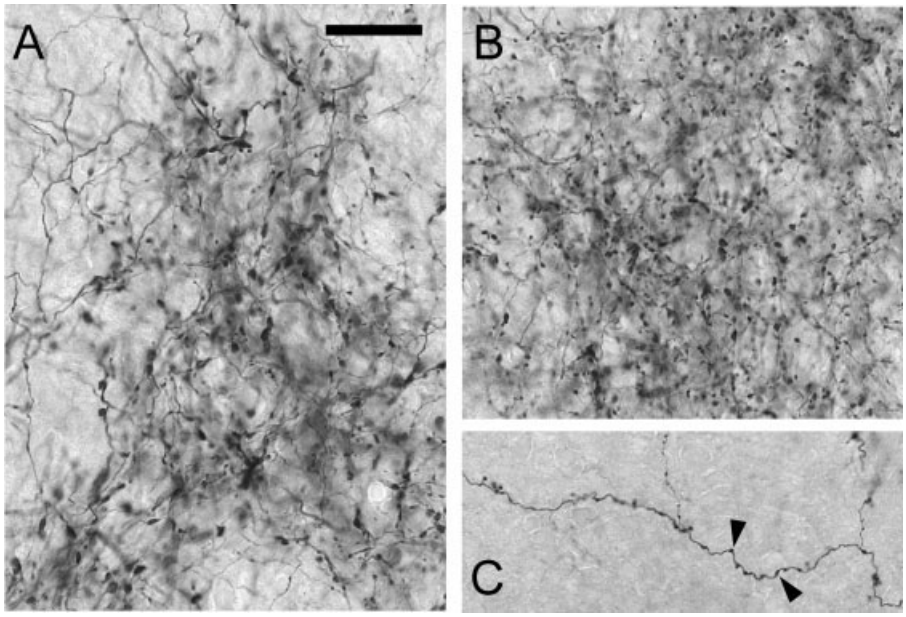

Fig. 10. Different size and morphology of terminal varicosities in EGFP-positive axons. **A:** Example of large varicosities (size rated 3 in Table 1) in the paracentral nucleus of the thalamus; this density of innervation is rated 4 in Table 1. **B:** Example of small and medium-sized varicosities (size rated 1-2 in Table 1) in the parafascicular nucleus. This density of innervation is rated 5 in Table 1. **C:** An isolated axon making "boutons en-passant" (arrowheads) in the cingulate cortex. Scale bar = 20 μm.

ergic neurons throughout the diencephalon and telencephalon. Therefore, the dense glycinergic innervation in these regions is of extrinsic origin. This conclusion is of major significance for understanding the role of inhibitory neurotransmission in the forebrain. In particular, the dense glycinergic innervation of thalamic intralaminar nuclei (Table 1) is likely to play a major role in the generation of low-threshold calcium spikes in these neurons, and therefore to modulate the rhythmic activity of the thalamocortical system. The visualization of preterminal EGFP-positive axons in the midbrain and entering the hypothalamus along the medial forebrain bundle strongly suggests that glycinergic axons innervating the forebrain originate from pontine or medullary levels.

The contribution of the glycinergic system to the cerebral cortex, hippocampus, amygdala, olfactory bulb, and striatum appears limited, although isolated axons were seen in all these structures, sometimes with a distinct area or laminar specificity, as illustrated in Figure 9. Glycine is therefore unlikely to play a major role as a neurotransmitter in these regions, although inhibitory control of specific pathways, such as in the stratum lacunosum-moleculare of the hippocampus, cannot be excluded.

Functional significance

The main function of GlyT2 is to ensure glycine supply of presynaptic terminals and, thereby, sufficient loading of synaptic vesicles by the vesicular inhibitory neurotransmitter transporter (Gomeza et al., 2003). This function is essential for postnatal survival in mice. Inactivation of GlyT2 by homologous recombination has revealed a severe phenotype, characterized by spasticity, muscular rigidity, tremor, and impaired righting responses (Gomeza et al., 2003). This phenotype might imply changes in glycinergic transmission at multiple levels, based on the present results, including the cerebellum, thalamus, and basal forebrain in addition to the spinal cord. Similar evidence for an important contribution of glycine to a variety of CNS functions comes from experiments with strychnine, a competitive antagonist at inhibitory glycine receptors, and from mice carrying mutations in glycine receptor genes (Legendre, 2001). Both approaches clearly indicate important roles for glycine not only in spinal motor control but also in sensory processing. Mice with inborn deficits in inhibitory glycine receptors show increased auditory startle responses (Koch et al., 1996) and are extremely sensitive to even light touch (White and Heller, 1982). Two recent studies now point to a key role of glycine in the spinal pain-controlling circuits. Prostaglandin E_2 (PGE_2), a pivotal mediator of inflammatory pain sensitization not only in peripheral tissues but also in the spinal cord, specifically inhibits glycine receptors located in the superficial laminae of the spinal cord dorsal horn (Ahmadi et al., 2002), where most nociceptive afferent nerve fibers terminate. This inhibition involves protein kinase A (PKA)-dependent phosphorylation of a specific glycine receptor subunit, α3, which is distinctly expressed in the superficial dorsal horn (Harvey et al., 2004). Mice lacking this glycine receptor subunit show a drastic reduction in the spinal pronociceptive effects of PGE_2 and significantly reduced inflammatory hyperalgesia. These findings led us to propose that PGE_2 causes central pain sensitization by disinhibiting the propagation of nociceptive signals through the spinal cord dorsal horn to higher brain areas where pain becomes conscious. This idea, however, requires that PGE_2 reduced glycinergic inhibition primarily of excitatory neurons (and spared inhibitory interneurons). Experiments performed in slices obtained from our GlyT2-EGFP mice indeed demonstrated that inhibition of glycinergic inhibitory postsynaptic currents (IPSCs) by

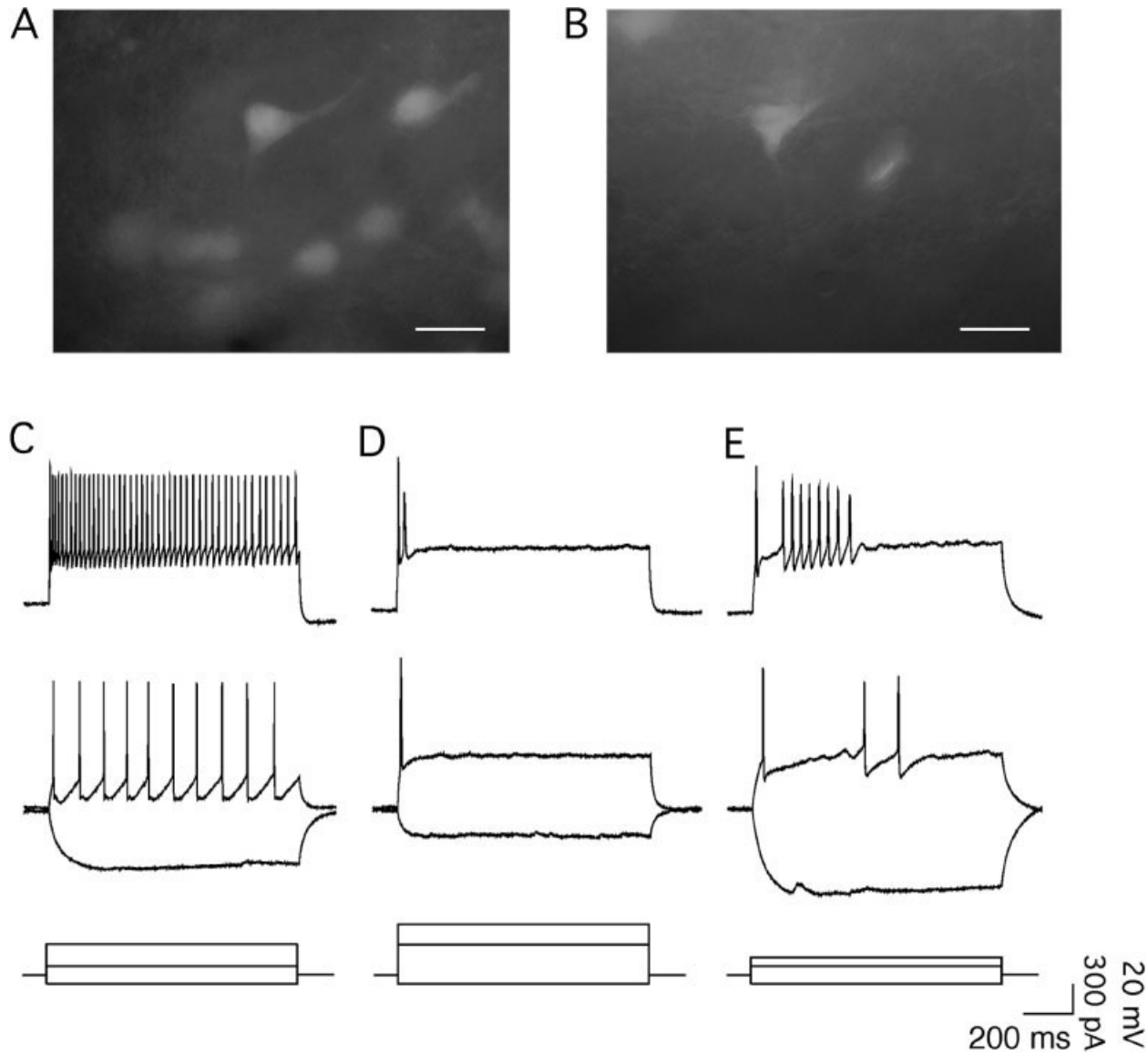

Fig. 11. Firing patterns of EGFP-positive and -negative neurons in the spinal cord dorsal horn. **A,B:** EGFP-positive neurons photographed in 250-μm-thick slices located at the border of laminae II and III (A) and in lamina I (B) were visualized with conventional fluorescence equipment with a ×60 water-immersion objective. Images were recorded with a CCD camera. **C–E:** Action potentials were elicited by depolarizing current injections (bottom). Tonic firing pattern (C) and single action potential firing (D) in two EGFP-positive neurons. E: EGFP-negative neuron, which showed phasic action potential firing with a gap after the first action potential. Scale bars = 10 μm.

TABLE 2. Electrophysiological Properties of Glycinergic and Nonglycinergic Neurons in the Superficial Laminae (I–III) of the Mouse Spinal Cord Dorsal Horn[1]

	Resting membrane potential (mV)	membrane input resistance (MΩ)	AP frequency (Hz)	AP threshold (mV)	AP amplitude (mV)	AP half width (msec)	AP overshoot (mV)	AP afterhyperpolarization (mV)
Glycinergic (n = 28)	−48.6 ± 2.8	270 ± 36	24.4 ± 2.8 (n=20)	−41.8 ± 1.7	55.5 ± 2.2	2.4 ± 0.4	15.1 ± 1.7	7.9 ± 0.6
Nonglycinergic (n = 22)	−52.4 ± 3.3	234 ± 25	14.4 ± 2.3 (n=20)	−41.4 ± 1.6	56.8 ± 2.4	2.2 ± 0.2	16.8 ± 1.4	8.2 ± 0.6

[1]AP firing frequency was determined during injection of −500 pA.

TABLE 3. Firing Properties of Glycinergic and Nonglycinergic Neurons Located in the Superficial Laminae (I–III) of the Mouse Spinal Cord Dorsal Horn[1]

	Tonic (%)	Single (%)	Phasic (%)	Delayed (%)
Glycinergic (n = 28)	15 (54)	9 (32)	3 (11)	1 (4)
Non-glycinergic (n = 22)	13 (59) (1 with gap)	4 (18)	4 (18) (1 with gap)	1 (5)

[1]Although single-firing neurons appear to be more prevalent among glycinergic neurons, differences remained below significance ($\chi^2 = 1.51$, n = 50, $P = (0.68)$. Tonic-firing neurons fired action potentials at frequencies of 23.4 ± 3.0 Hz (glycinergic neurons, n = 15) and 23.9 ± 1.8 Hz (nonglycinergic neurons, n = 13).

PGE_2 was much less in glycinergic neurons than in nonglycinergic, neighboring neurons (Zeilhofer et al., 2003). Glycinergic neurons thus possess specific pharmacological properties beyond their glycinergic phenotype that distinguish them from nonglycinergic neurons. The detailed functional analysis of glycinergic neurons in brain slices or even in vivo with the use of laser-guided recording techniques (Margrie et al., 2003) will greatly benefit from the generation of these mice. The latter is particularly significant because our study has shown that firing patterns cannot be used as reliable markers for the identification of glycinergic neurons in slice preparations.

ACKNOWLEDGMENTS

The authors thank Drs. David Pow and Detlev Boison for a generous supply of antibodies; Dr. Uwe Rudolph for initial helpful suggestions; and Ruth Keist, Corinne Sidler, and Franziska Parpan for excellent technical assistance.

LITERATURE CITED

Adams RH, Sato K, Shimada S, Tohyama M, Püschel AW, Betz H. 1995. Gene structure and glial expression of the glycine transporter GlyT1 in embryonic and adult rodents. J Neurosci 15:2524–2532.

Ahmadi S, Lippross S, Neuhuber WL, Zeilhofer HU. 2002. PGE_2 selectively blocks inhibitory glycinergic neurotransmission onto rat superficial dorsal horn neurons. Nat Neurosci 5:34–40.

Antal M, Petko M, Polgar E, Heizmann CW, Storm-Mathisen J. 1996. Direct evidence of an extensive GABAergic innervation of the spinal dorsal horn by fibres descending from the rostral ventromedial medulla. Neuroscience 73:509–518.

Araki T, Yamano M, Murakami T, Wanaka A, Betz H, Tohyama M. 1988. Localization of glycine receptors in the rat central nervous system: an immunocytochemical analysis using monoclonal antibody. Neuroscience 25:613–624.

Borowsky B, Mezey E, Hoffmann BJ. 1993. Two glycine transporter variants with distinct localization in the CNS and peripheral tissues are encoded by a common gene. Neuron 10:851–863.

Freund TF, Buzsaki G. 1996. Interneurons of the hippocampus. Hippocampus 6:345–470.

Gomeza J, Ohno K, Hülsmann S, Armsen W, Eulenburg V, Richter DW, Laube B, Betz H. 2003. Deletion of the mouse glycine transporter 2 results in a hyperekplexia phenotype and postnatal lethality. Neuron 40:797–806.

Gong S, Zheng C, Doughty ML, Losos K, Didkovsky N, Schambra UB, Nowak NJ, Joyner A, Leblanc G, Hatten ME, Heintz N. 2003. A gene expression atlas of the central nervous system based on bacterial artificial chromosomes. Nature 425:917–925.

Harvey RJ, Depner UB, Wässle H, Ahmadi S, Heindl C, Reinold H, Smart TG, Harvey K, Schütz B, Abo-Salem OM, Zimmer A, Poisbeau P, Welzl H, Wolfer DP, Betz H, Zeilhofer HU, Müller U. 2004. GlyR α3: an essential target for spinal PGE2-mediated inflammatory pain sensitization. Science 304:884–887.

Heintz N. 2001. Bac to the future: the use of BAC transgenic mice for neuroscience research. Nat Rev Neurosci 2:861–870.

Jursky F, Nelson N. 1995. Localization of glycine neurotransmitter transporter (GLYT2) reveals correlation with the distribution of glycine receptor. J Neurochem 64:1026–1033.

Koch M, Kling C, Becker CM. 1996. Increased startle responses in mice carrying mutations of glycine receptor subunit genes. Neuroreport 7:806–808.

Legendre P. 2001. The glycinergic inhibitory synapse. Cell Mol Life Sci 58:760–793.

Liu QR, Lopez-Corcuera B, Mandiyan S, Nelson H, Nelson N. 1993. Cloning and expression of a spinal cord- and brain-specific glycine transporter with novel structural features. J Biol Chem 268:22802–22808.

Malosio ML, Marqueze-Pouey B, Kuhse J, Betz H. 1991. Widespread expression of glycine receptor subunit mRNAs in the adult and developing rat brain. EMBO J 10:2401–2409.

Margrie TW, Meyer AH, Caputi A, Monyer H, Hasan MT, Schaefer AT, Denk W, Brecht M. 2003. Targeted whole-cell recordings in the mammalian brain in vivo. Neuron 39:911–918.

Meyer AH, Katona I, Blatow M, Rozov A, Monyer H. 2002. In vivo labeling of parvalbumin-positive interneurons and analysis of electrical coupling in identified neurons. J Neurosci 22:7055–7064.

Ponce J, Poyatos I, Aragon C, Gimenez C, Zafra F. 1998. Characterization of the 5′ region of the rat brain glycine transporter GLYT2 gene: identification of a novel isoform. Neurosci Lett 242:25–28.

Pow DV, Wright LL, Vaney DI. 1995. The immunocytochemical detection of amino-acid neurotransmitters in paraformaldehyde-fixed tissues. J Neurosci Methods 56:115–123.

Poyatos I, Ponce J, Aragon C, Gimenez C, Zafra F. 1997. The glycine transporter GLYT2 is a reliable marker for glycine-immunoreactive neurons. Brain Res Mol Brain Res 49:63–70.

Rampon C, Luppi PH, Fort P, Peyron C, Jouvet M. 1996. Distribution of glycine-immunoreactive cell bodies and fibres in the rat brain. Neuroscience 75:737–755.

Ruscheweyh R, Ikeda H, Heinke B, Sandkühler J. 2004. Distinctive membrane and discharge properties of rat spinal lamina I projection neurones in vitro. J Physiol 555:527–543.

Smith KE, Borden LA, Hartig PR, Branchek T, Weinshank RL. 1992. Cloning and expression of a glycine transporter reveal colocalization with NMDA receptors. Neuron 8:927–935.

Spike RC, Watt C, Zafra F, Todd AJ. 1997. An ultrastructural study of the glycine transporter GLYT2 and its association with glycine in the superficial laminae of the rat spinal dorsal horn. Neuroscience 77:543–551.

Tanaka I, Ezure K. 2004. Overall distribution of GLYT2 mRNA-containing versus GAD67 mRNA-containing neurons and colocalization of both mRNAs in midbrain, pons, and cerebellum in rats. Neurosci Res 49: 165–178.

Todd AJ, Sullivan AC. 1990. Light microscope study of the coexistence of GABA-like and glycine-like immunoreactivities in the spinal cord of the rat. J Comp Neurol 296:496–505.

van den Pol AN, Gorcs T. 1988. Glycine and glycine receptor immunoreactivity in brain and spinal cord. J Neurosci 8:472–492.

White WF, Heller AH. 1982. Glycine receptor alteration in the mutant mouse spastic. Nature 298:655–657.

Yang XW, Model P, Heintz N. 1997. Homologous recombination based modification in Escherichia coli and germline transmission in transgenic mice of a bacterial artificial chromosome. Nat Biotechnol 15:859–865.

Zafra F, Aragon C, Gimenez C. 1997. Molecular biology of glycinergic neurotransmission. Mol Neurobiol 14:117–142.

Zafra F, Aragon C, Olivares L, Danbolt NC, Gimenez C, Storm-Mathisen J. 1995. Glycine transporters are differentially expressed among CNS cells. J Neurosci 15:3952–3969.

Zeilhofer HU, Studler B, Arabadzisz D, Ahmadi S, Layh B, Boesl MR, Fritschy JM. 2003. Glycinergic neurons expressing EGFP in BAC transgenic mice. Program No. 888.18. 2003 Abstract Viewer/Itinerary Planner. Washington, DC: Society for Neuroscience. Available online.